2016

Cellular Consequences of Lysosomal Rupture Induced by Alpha Synuclein

Zachary Carpenter Green
Loyola University Chicago

LOYOLA UNIVERSITY CHICAGO

CELLULAR CONSEQUENCES OF LYSOSOMAL RUPTURE INDUCED BY ALPHA SYNUCLEIN

A THESIS SUBMITTED TO
THE FACULTY OF THE GRADUATE SCHOOL
IN CANDIDACY FOR THE DEGREE OF
MASTER OF SCIENCE

PROGRAM IN NEUROSCIENCE

BY
ZACHARY C. GREEN
CHICAGO, ILLINOIS
AUGUST 2016

TABLE OF CONTENTS

LIST OF FIGURES

ABBREVIATIONS

ALP	Autophagy-lysosome pathway
α-syn	Alpha Synuclein
BFA	Bafilomycin A1
CMV	Cytomegalovirus
CNS	Central nervous system
Cyt-C	Cytochrome C
EMCCD	Electron-multiplying charge coupled device
FACS	Fluorescence activated cell sorting
GFP	Green fluorescent protein
LB	Lewy body
LLOMe	L-Leucyl-L-leucine methyl ester
LN	Lewy neurite
MSA	Multiple system atrophy
NHS	N-hydroxysuccinimide
PBS	Phosphate-buffered saline
PCR	Polymerase chain reaction
PD	Parkinson's disease
PIPES	Piperazine-N,N'-bis-(2-ethanesulfonic acid)
NDS	Normal donkey serum
NT	No treatment
ROS	Reactive oxygen species
SDS-PAGE	Sodium dodecyl sulfate polyacrylamide gel electrophoresis
Ser-129	Serine Residue 129
SNAP	Soluble NSF Attachment Protein
SNARE	SNAP receptor
SNP	Single nucleotide polymorphism

TNFα	Tumor necrosis factor alpha
TIRF-M	Total internal reflection microscopy
VSVg	Vesicular stomatitis virus glycoprotein G

CHAPTER ONE

OVERVIEW AND HYPOTHESES

Misfolded, toxic forms of the amyloid protein, alpha synuclein (α-syn), have been implicated in Parkinson's disease (PD) pathology and have been shown to spread throughout the brain in a prion-like manner, explaining the characteristic, progressive loss of dopaminergic neurons in PD[1–3]. A major barrier to identifying targets for more impactful treatment of PD is the lack of mechanistic understanding behind this process of α-syn propagation. Mechanisms currently being investigated include those behind cellular release, uptake, and intracellular processing of α-syn aggregates[4]. Evidence suggests that exogenous α-syn aggregates can enter recipient cells through the endocytic pathway to subsequently induce endocytic vesicle rupture, resulting in the cytosolic deposition of exogenous α-syn aggregates[5–7]. More specifically, previous colocalization studies in our lab provide evidence that α-syn induced vesicle rupture, labeled by recruitment of overexpressed mCherry-Galectin 3 (chGal3) to exposed beta-galactoside sugars located exclusively at the site of rupture, occurs mainly at the lysosomal stage of the endocytic pathway[7].

Moving forward, we have aimed to corroborate this previous evidence of α-syn induced lysosomal rupture, and to investigate the cellular repercussions of this rupture with respect to cell death and α-syn transfer. We hypothesized that α-syn aggregates can compromise the function of lysosomes, leading to the release of lysosomal contents, including key hydrolytic enzymes, into the cytosol. To test this, we have immunofluorescently labeled one of the most abundant lysosomal proteolytic enzymes, cathepsin B, to analyze the level of lysosomal protease dispersion upon treatment with α-

syn aggregates in **aim 1**. Further, we hypothesized that ruptured lysosomes would be incapable of resealing after α-syn induced rupture. We have tested this hypothesis in **aim 2** using a triple colocalization analysis between live cell lysosomal markers, labeled α-syn aggregates, and chGal3 labeled rupture events. Last, we hypothesized that membrane-proximal, endocytic lysosomes and autolysosomes may undergo calcium-dependent lysosomal exocytosis to release their α-syn contents prior to rupture. In **aim 3**, we have investigated this mechanism of α-syn release by inducing calcium influx while imaging membrane proximal lysosomes and their contents through TIRF-M.

CHAPTER TWO

REVIEW OF LITERATURE

PD Pathology, Symptoms, and Treatments

The aberrant accumulation of α-syn amyloid structures within the brain is increasingly acknowledged as the underlying cause of PD. As α-syn continues to aggregate, inclusions are formed within CNS cell bodies or axons that are referred to as Lewy bodies (LBs) or Lewy neurites (LNs) respectively, and are the common histopathological feature of all synucleinopathies including PD, DLB, and MSA[8–13]. Advancing α-syn pathology leads to the progressive loss of neuronal and glial cell populations through unconfirmed mechanisms, giving rise to the distinct neurological symptoms of each synucleopathy[14,15]. Although the involvement of α-syn inclusions is a universal feature of these synucleinopathies, each disease within this category is characterized differently and tends to involve distinct brain regions, cell types, symptoms, and time courses for disease progression. MSA is one of the most distinct synucleinopathies in that it is diagnosed after discovery of extensive Lewy body structures within glial tissue, and is characterized by massive glial scarring in autonomic centers of the brain, giving rise to many symptoms including dysphagia and severe respiratory dysfunction[13,16,17]. Alternatively, PD is characterized by the death of dopaminergic neurons within the Substantia Nigra pars compacta (SNpc) of the midbrain, yet Lewy body and Lewy neurite structures can be found throughout the CNS[18]. Further, the intricacies of α-syn pathology in PD patients can vary significantly as different brain regions are affected, giving rise not only to the cardinal signs of bradykinesia, resting tremor, rigidity, and impaired postural instability, but also an array

of secondary symptoms including loss of olfaction and cognitive deficits[19,20]. The eventual spread of pathology throughout cortical areas may explain the high instances of dementia known as PDD, which affects approximately 26% of PD patients at initial diagnosis, and 78% at 8 years after diagnosis[21]. The characteristics of PDD are similar to those of DLB, where cortical areas are the most drastically affected by neuronal death, yet the amyloid deposits of α-syn in DLB are much more prevalent and develop throughout the CNS much more quickly than those found in patients with PD/PDD[22]. This may explain why, from the time of diagnosis, the average life expectancy in DLB is just 5 years compared to the 9 year life expectancy after onset of PD[23].

Current treatments for PD and all synucleinopathies revolve around temporary symptom management and do not prevent disease progression through neuronal loss. The standard of care for PD includes treatment with L-DOPA, a precursor that can cross the BBB and be converted into dopamine by DOPA decarboxylase, thereby enhancing neurotransmission from dopaminergic SNpc neurons to the dorsal striatum[24]. After pharmacological treatments begin to fail and produce complications like worsening dyskinesia, qualifying PD patients can undergo surgical implantation of an electrode stimulator, normally into the subthalamic nucleus, to inhibit abnormal neural activity associated with motor dysfunction[25]. Although deep brain stimulation (DBS) drastically improves motor symptoms and life expectancy, eventually, even DBS treatment fails to alleviate movement associated symptoms[25]. More importantly, these treatments have limited effect on the non-motor symptoms of PD (cognitive impairment, speech deficits, pain, imbalance, etc.), and, for that reason, is currently only indicated as a treatment for motor symptoms[26]. Additional treatments that may become publically available in the near

future include grafting of stem cells to replace dying SNpc dopaminergic neurons, although this approach also does not address the underlying pathology[27].

Origin of Pathology

It has been well established that dopaminergic neurons within the SNpc undergo selective, accelerated loss in PD, but the explanation for this phenomenon is still largely debated. Despite the selective damage to SNpc neurons, aberrant α-syn aggregation is commonly thought to originate in other areas of the CNS or possibly the periphery, such as the dorsal motor nucleus, glossopharyngeal nerve, vagal nerve, the anterior olfactory nucleus, or even the enteric nervous system within the GI tract[14,28]. Those who accept the Braak hypothesis believe that α-syn pathology spreads in a predictable manner throughout the CNS, entering the brain through the brainstem from peripheral origination sites[14]. However, the previously mentioned wide spectrum of symptoms associated with PD suggests that spreading pathology may be unique in many cases and therefore difficult to predict. Various additional patterns of spreading pathology have also been recorded, including the observation that LNs are initially larger and more prevalent than LBs.[14]

Properties of Alpha Synuclein

Synuclein proteins are expressed systemically under normal conditions, but they are most abundant within the CNS where they can comprise as much as 1% of the total cytosolic protein content[29]. Within the cytosol, α-syn is localized to the synaptic termini and the nuclear envelope, explaining the origin of the name 'synuclein'[30,31]. In its free cytosolic form, α-syn is soluble, monomeric, and unfolded with no secondary structure, although contact with lipid membranes will cause α-syn to adopt an amphipathic alpha helical structure, most likely through hydrophobic interactions[32]. This dichotomy of α-syn

structure has led to investigation into the potential role of α-syn in vesicle trafficking; a line of thinking that has thus far proved to be accurate. Most notably, a recent study from Burré et al suggests that α-syn forms multimers of the helical structure while in contact with vesicle membranes, and is essential to the formation of SNARE complex proteins[33].

Alternatively, in states of synucleopathy, α-syn misfolds to form amyloid, filamentous structures containing phosphorylated α-syn beta-sheets[34–36]. Once amyloid structures form, they are strongly resistant to degradation by proteinases[37]. Perplexingly, initial misfolding seems to have little genetic influence since the WT form of α-syn is involved in 80% of PD cases, which are considered sporadic, while genetic variations (SNPs, duplications, and triplications) are known to promote early onset PD in the other 20% of cases. It has been proposed that particular point mutations may promote formation of LBs and LNs by destabilizing the functional helical structure of α-syn, thereby increasing the probability of the protein adopting an amyloid structure[32]. Studies investigating duplications and triplications of the SNCA gene, on the other hand, have shown that simply overexpressing α-syn will promote development of amyloid pathology[38,39]. Beyond these fairly rare genetic variations in the SNCA gene, age is the greatest known risk factor for PD, as is the case for so many neurodegenerative diseases.

Exogenous Alpha Synuclein Uptake and Vesicle Rupture

Pathological forms of α-syn have been detected extracellularly (e.g. CSF, plasma) in individuals with PD, evidence of α-syn translocation from the cytosol[40–42]. As these extracellular α-syn aggregates come into contact with the external leaflet of recipient cell plasma membranes, they are known to induce endocytosis, although the specific mechanism of endocytosis remains unknown[43]. This mechanism of cellular entry is very

similar to that of other pathogens, namely adenovirus. In order to fully progress through the viral life cycle after endocytosis, adenovirus must escape the endocytic pathway prior to degradation within lysosomes. Studies performed by Dr. Chris Wiethoff at Loyola suggest that adenovirus effectively evades degradation by inducing endocytic vesicle rupture to gain access to the cytosol. Vesicular rupture events in this and other recent studies were measured through the overexpression of a fusion protein, mCherry-Galectin 3 (chGal3)[44,45]. Cells were transduced to stably overexpress chGal3 based on the affinity of the Galectin 3 carbohydrate recognition domain for beta-galactoside sugars present exclusively on the extracellular surface, and the topologically equivalent interior leaflet of endocytic vesicle membranes[46] (**Figure #1-i**). When vesicle rupture occurs, these sugars become exposed to the cytosol where chGal3 is diffusely localized, allowing chGal3 to be recruited to form punctuates which can be measured above background fluorescence as individual rupture events (**Figure #1-ii**).

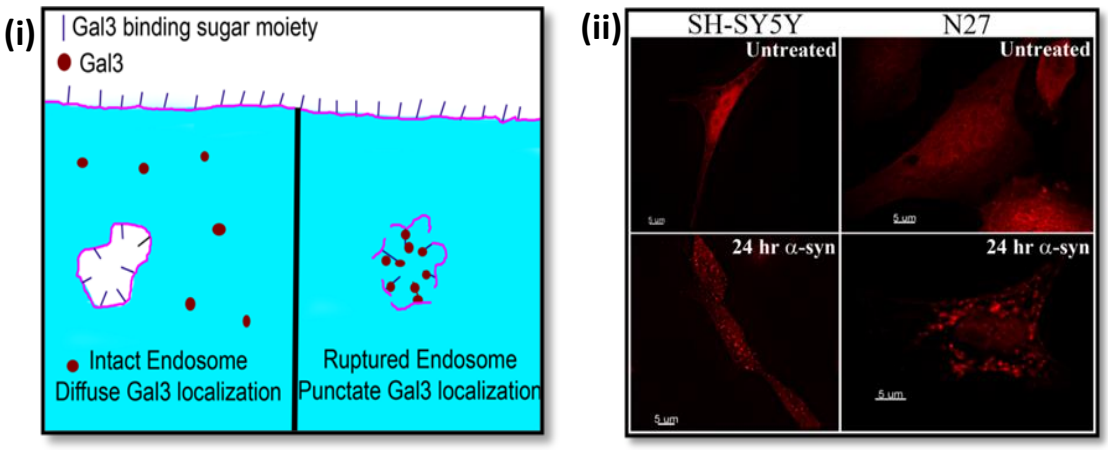

Figure 1. Schematic of the chGal3 labeled rupture system. Overexpressed Cherry-Galectin 3 (chGal3) is diffusely localized under normal conditions. After vesicle rupture occurs, chGal3 binds exposed sugars to form punctuates. (i) Illustrated depiction of chGal3 re-localization. (ii) Fluorescent images of two different neuronal cell types depicting chGal3 re-localization as a result of treatment with α-syn aggregates.

Further studies from the Wiethoff lab using this chGal3 assay system suggest that induction of vesicle rupture, in the context of adenovirus, is dependent on adenoviral protein VI[47]. Protein VI is thought to induce this membrane rupture by exerting a biomechanical tension on the membrane, achieved through interaction between the curved N-terminal, amphipathic α-helical structure of the protein and the vesicle membrane[47]. This induced rupture event in the context of adenovirus has been shown to occur more frequently at early stages along the endocytic pathway, particularly at the stage of the early endosomes[44]. Using the same assay system for vesicle rupture, we have been able to begin characterizing similar rupture events induced by α-syn.

Just like the adenovirus, α-syn adopts an N-terminal amphipathic α-helical structure in association with lipid membranes[48–50]. Yet, misfolded α-syn does not seem to exhibit the same evolutionarily driven, early escape from the endocytic pathway. Instead, our studies suggest that α-syn is likely to progress along the endocytic pathway until the inhabited vesicle matures to become an acidified lysosome, containing active proteases[7]. Alpha synuclein has been shown to induce rupture preferentially at this lysosomal stage of endocytosis[7]. Moreover, our studies show that α-syn aggregates can progress through the endocytic pathway to induce lysosomal rupture within a 24 hour time period[7]. This would not only explain the ability of α-syn to form Lewy body structures in the cytosol of recipient cells, but also may explain the ability of α-syn aggregates to induce cell death since lysosomal rupture will trigger the release of active proteases which are capable of activating pro-apoptotic pathways. Through the quantification of active caspase-3, apoptotic activation as a result of vesicle rupture in models of PD has become a major area of investigation[7,51,52].

Cathepsin Dispersion Following Lysosomal Rupture

The link between endocytic vesicle rupture and caspase-3 related cell death is likely to involve dispersion of hydrolytic enzymes from the lysosomal compartment (**Figure #2**). Of the many hydrolytic enzymes contained within the lysosomal lumen, the aspartic and cysteine cathepsins, cathepsin D and cathepsin B respectively, are known to be most abundant within lysosomes and have also been implicated in the activation of various cell death pathways upon aberrant release into the cytosol[53–56].

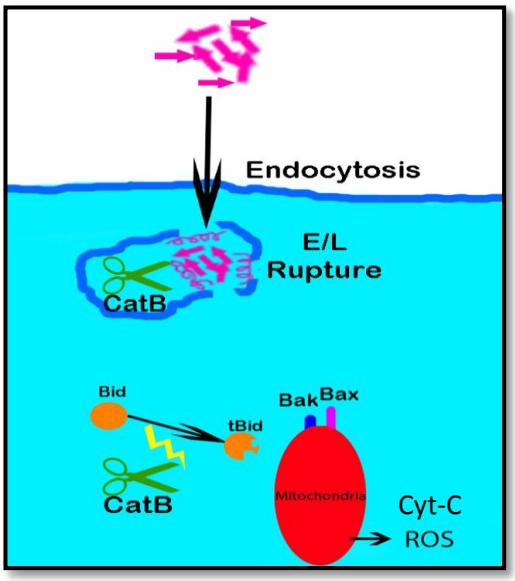

Figure 2. Model of α-syn induced cell death through lysosomal rupture and cathepsin release.

Cathepsin D is responsible for activating many of the cysteine cathepsins in the acidic environment of the lysosomal lumen, but cathepsin B undergoes autocatalytic activation through the cleavage of its own N-terminal propeptide under lysosomal conditions[57]. The subsequent release of active cathepsin B under pathological conditions is particularly threatening to intracellular environment due to the unique ability of cathepsin B to remain significantly active at neutral pH, especially when bound to naturally occurring heparin[58,59]. Once released, cathepsin B has not only been shown to necrotically degrade

tissue, but also to activate apoptotic pathways through the cleavage of Bid, a Bcl-2 family protein, to form the active ligand, tBid[52,53,57,58]. After tBid is produced, it can initiate downstream activation of the apoptisome. This is accomplished by tBid after allosteric activation of Bak, subsequent Bak/Bax oligomerization, and release of Cyt-C through the Bak/Bax channel on the outer mitochondrial membrane[53]. The same oligomerization and outcome can also be induced in the opposite manner when cathepsin D is released to activate Bax[54]. Following oligomerization of Bax and Bak, reactive oxygen species are released from the mitochondria, ultimately leading to phosphorylation of α-syn at Ser-129 and subsequent enhancement of α-syn aggregation to form Lewy body structures, although the specific kinases involved have yet to be identified[34,60,61]. This sequence of cellular events could explain the currently undescribed pathway of cell death in PD, and could shed light on potential mechanisms of α-syn propagation. For these reasons, the localizations of both cathepsin D and cathepsin B within models of PD have become a key interest.

Multiple studies provide compelling evidence that both lysosomal and mitochondrial dysfunctions are associated with PD pathology[53,60,62–64]. We believe that cathepsin dispersion due to α-syn induced lysosomal rupture could explain both of these implicated types of dysfunction. However, the cellular repercussions of cathepsin release can be variable depending on the extent to which cathepsin release occurs[55]. Lysosomes that become moderately permeabilized over time to release small amounts of active cathepsins may selectively induce apoptosis through Bax/Bak activation, while full rupture of lysosomes to release high concentrations of cathepsins can result in unregulated necrosis[55]. If necrosis is induced in PD, damage would not only occur within the cell of pathological origin, but a loss of cell membrane integrity could feasibly enhance the

propagation of PD pathology by allowing additional release of α-syn aggregates for uptake by neighboring cells. Determining the role of aberrant cathepsin release in the progression of PD will be instrumental in the identification of degenerative pathways, mechanisms of intercellular propagation, and eventual therapeutic targets.

Seeding of endogenous alpha synuclein

In addition to cathepsin dispersion, exogenous α-syn aggregates can likely be released into the cytosol after rupture of the endocytic vesicle. This vesicular escape could allow exogenous aggregates to contribute to the formation of LB structures within the cytosol by serving as nucleation points not only for other exogenous α-syn aggregates, but for endogenous α-syn that has yet to misfold[65]. This occurrence has been described by multiple groups, including Brundin et al, who conducted studies demonstrating that endogenously overexpressed human α-syn can transfer from donor to recipient cells in a time dependent manner in vitro, and to grafted dopaminergic neurons in animal models to seed further formation of LBs and LNs[3,65,66]. More importantly, this type of transfer has been shown to induce measurable decreases in both viability and striatal fiber density of grafted neurons[67,68].

Alpha Synuclein Release

The Brundin lab is one of many that have contributed to the extensive repertoire of studies supporting the prion hypothesis of α-synuclein propagation. Additional studies from the Seung-Jae Lee lab at Konkuk University have provided evidence of in vitro transfer that is enhanced by inhibition of autophagy, while the Kordower lab at Rush University has reported transfer upon post-mortem analysis of clinically grafted neurons[27,69]. Although all of these studies provide fantastic evidence that α-syn transfer

can occur, very little progress has been made toward understanding the underlying mechanisms of α-syn release. Perhaps the only major mechanistic finding to date is that standard secretory mechanisms of α-syn release can be ruled out due to persisting release after inhibition of secretory vesicle formation by treatment with BFA[70]. This lack of knowledge makes mechanistic study of α-syn release an extremely important, yet demanding and unsupported area of study. In order to make progress, pilot studies must be performed to investigate feasible alternatives.

Role of Intracellular Calcium in Alpha Synuclein Transfer

The process of calcium-dependent exocytosis is extremely well studied and normally involves interactions between intracellular vesicles and the inner leaflet of the plasma membrane through SNARE protein complex formation[71]. Secretory and synaptic vesicles are guided to target destinations by specific membrane bound Rab GTPases which interact with cytoskeletal-associated motor proteins to facilitate transport[72]. Upon arrival at the target site, vesicular SNARE protein interacts with t-SNARE on the inner leaflet of the plasma membrane, followed by formation of the full SNARE complex. Once the SNARE complex is formed, vesicles are docked and primed, awaiting calcium influx and binding to synaptotagmin calcium sensor proteins as the final signal to initiate fusion and release of vesicle contents into the extracellular space.

More recently, it has been established that membrane proximal lysosomes are capable of undergoing exocytosis through the same mechanism. In fact, there is evidence to suggest that lysosomes are the predominant intracellular vesicle species to undergo calcium dependent exocytosis in non-secretory cells, and that all cells utilize lysosomal exocytosis for a variety of functions, including membrane repair and cell response to

invading pathogens[73–76]. In lysosomes, exocytosis is facilitated by the calcium sensor, synaptotagmin VII, and is has been associated with the release of lysosomal contents into the extracellular space[58,73,75,77,78]. Since lysosomes often contain α-syn aggregates[79], the tendency for lysosomes to undergo exocytosis in response to calcium influx implicates lysosomal exocytosis as a potential release mechanism for α-syn aggregates.

Misfolded forms of α-syn can be directed into the lumen of lysosomes through either the endocytic pathway, if the aggregates are exogenous in origin, or through the autophagy-lysosome pathway (ALP) as the cell attempts to sequester and degrade increasing levels of aberrant, endogenous aggregates from the cytosol under pathological conditions[80]. Further, α-syn aggregates are known to cause dysfunction within the ALP, the consequences of which are enhanced α-syn accumulation within lysosomes and increased release of α-syn aggregates from cells[69,80]. This increased release of α-syn aggregates caused by ALP dysfunction has proven to cause cellular consequences, as it has been directly linked to increased apoptosis in neighboring cells through the measurement of caspase-3 activation[69].

If α-syn is known to accumulate in lysosomes, and cannot be released through standard secretory mechanisms, perhaps lysosomal exocytosis is a feasible mechanism of propagation. Recent thought-provoking studies have successfully demonstrated a calcium-dependent release of uncharacterized exosomes containing α-syn, presumably being released from cells through the fusion of MVBs with the plasma membrane. Nonetheless, somewhat contrasting studies provide evidence to suggest that free aggregates of α-syn are also often released into the extracellular space[69,81]. A possible explanation for this collection of findings is the proposed model on page #41, in which lysosomal exocytosis

can explain the calcium-dependent release of both vesicular and free α-syn aggregates depending on the trafficking of α-syn through the endocytic and autophagy-lysosome pathways (**Figure #16**).

Using TIRF microscopy, we aimed to determine whether calcium dependent lysosomal exocytosis may play a role in α-syn release and propagation. Calcium influx was induced by treatment with various ionophores, namely calcium ionophores A23187 and calcium ionomycin[73,81]. We hypothesized that calcium influx would induce lysosomal migration and fusion to the PM, resulting in a corresponding increase in visible α-syn release from neuronal cell lines in vitro.

Significance of this Study

The significance of our overall study is that it aims to identify novel therapeutic targets related to the propagation of pathology in not only PD, but many related synucleinopathies. If our findings contribute to an improved understanding of α-syn toxicity, intracellular trafficking, and release, then the direction of current research may pivot from symptom management approaches to propagation prevention with the potential of entirely halting disease progression in relevant synucleinopathies.

CHAPTER THREE

MATERIALS & METHODS

Cell culture

The SH-SY5Y human neuroblastoma cell line was acquired from the American Type Culture Collection (ATCC). Cells were cultured in Dulbecco's modified Eagle's Medium (DMEM) containing phenol red (Invitrogen) and supplemented with 10% fetal bovine serum (FBS), 10 ug/ml ciprofloxacin hydrochloride, 1,000 U/ml penicillin, and 1,000 U/ml streptomycin. For live cell imaging, DMEM lacking phenol red was used, and cells were both cultured and imaged in live cell microscopy Delta T Dishes (Bioptechs).

Overexpression of cherry-galectin 3

For vesicle rupture experiments, SH-SY5Y cells were transduced to stably overexpress chGal3 using a lentiviral viral vector (pLVX) containing the chGal3 gene under control of a CMV promoter. To generate lentivirus for transduction, HEK 293T cells were transfected using PEI as a transfection reagent with a mixture of equivalent parts VSVg, ΔNRF, and pLVX-CMV-chGal3 plasmid. Lentiviral particles were purified 24 hours post-transfection from conditioned media of 293T cells using a 0.45um Millipore syringe. SH-SY5Y cells were then cultured to 80% confluency, treated with the purified lentivirus, and spinoculated at 13°C for 2h at 1200 x g. The resulting SH-SY5Y chGal3 cells were selected using 5 ug/ml puromycin within the previously mentioned culture medium.

Alpha synuclein aggregation and labeling

Full length, recombinant α-syn aggregates for these experiments were generated by constant 3-day agitation of purified α-syn monomer in PBS, at a concentration of 5 mg/ml and a constant temperature of 37°C[82]. To prepare aggregates for fluorescence microscopy, they were labeled with DyLight™ 488 NHS-ester fluorophores (ThermoFisher). Oligomeric structure of aggregated α-syn was confirmed by EM, and was verified to have increased molecular weight compared to α-syn monomer by SDS- and native-PAGE. Cells in all studies were treated with α-syn aggregates for 24 hours, although concentrations were different for specific experiments, varying within the recommended 1ug/ml to 5ug/ml range of concentrations normally used for treatment with exogenous aggregates[82].

Immunofluorescent Staining

For cathepsin B dispersion experiments, cells were fixed in 0.1 M PIPES with 3.7% formaldehyde (Polysciences) at a pH of 6.8 for 20 minutes. Immediately after fixation, cells were incubated with one of two polyclonal, rabbit anti-cathepsin B antibodies (Abcam at 1ug/ml, or Santa Cruz at 0.5ug/ml), in a PBS solution containing 10% NDS, 0.1% Saponin, (Sigma-Aldrich) and 0.01% NaN3 for 1.5 hours. After primary staining, samples were fluorescently labeled with anti-Rabbit 576-conjugated secondary antibody at a concentration of 1:500, and DAPI (1ug/ml) for 20 minutes. Additional staining of vesicular antigens in control experiments was done under the same IF protocol using 1:400 mouse anti-EEA1 (BD Biosciences) and 1:400 mouse anti-LAMP-2 (BD Biosciences) followed by incubation with 1:500 488-conjugated anti-mouse secondary antibody (BD Biosciences).

Drug-induced vesicle rupture

As a positive control for lysosomal rupture and cathepsin B dispersion, cells were treated with 10mM LLOMe in DMEM for 1 hour, followed by replacement of drug containing media with standard media for a post-treatment incubation period of two hours before fixation. Cells were then fixed and stained for cathepsin B according to the above immunofluorescence protocol.

Wide-field fluorescence deconvolution microscopy

Immunofluorescence imaging was performed on a DeltaVision microscope (Applied Precision) fitted with a 12-bit CoolSNAP HQ digital camera (Photometrics) and 1.4-numerical aperture 100X objective lens.

Live-cell fluorescence images were generated for triple colocalization analysis with the same DeltaVision microscope and 100X objective lens, fitted with an alternate 16-bit Cascade 2 EMCCD digital camera (Photometrics). During imaging, cells were maintained within a Weather Station^{TM} chamber at 5% CO_2 and 37°C.

Resulting images in each study were deconvolved immediately after acquisition using the SoftWoRx deconvolution software (Applied Precision).

Analysis of deconvolved images

The analysis of resulting, deconvolved three-dimensional images was carried out within the Imaris software package (Bitplane). Surfaces were generated for channels of interest, and applied to all collected images using the high-throughput Batch Coordinator tool (Bitplane). Multiple parameters from the Batch output were considered, including both maximum fluorescence intensity and volume of generated surfaces for

colocalization analysis, or overall surface count for the quantification of fluorescent puncta abundance between treatment groups for the cathepsin B dispersion study.

Total internal reflection microscopy

To visualize calcium-dependent exocytosis of α-syn aggregates at the membrane of human neuronal cells, SH-SY5Y cells were plated onto Fibronectin (Sigma-Aldrich) coated 8-well, 1.0 Borosilicate chamber slides (ThermoFisher) and imaged using live cell, total internal reflection fluorescence microscopy. A Nikon TIRF microscope equipped with an EMCCD iXon 887 camera, computer-controlled automatic filter wheels (Sutter), 1.49 NA x 100 TIRF-optimized objective, and objective heating element. Labeled α-syn aggregates were excited by a 445 nm Argon laser passed through a 488-reflecting dichroic mirror optimized for TIRF (Semrock). For most experiments, the stream acquisition function of the Metamorph software package was used to take TIRF images focused on the bottom membrane of plated cells every 238 ms for an average duration of 180 seconds. In select experiments, filter automation was used to image chGal3 and 488-labeled α-syn in alternating 0.5 second intervals for an average duration of 180 seconds. Single epifluorescent images of the 488-labeled α-syn were taken before and after stream acquisition in all experiments. Before and after stream acquisition, chGal3 was excited by a Prior Lumen 200 broad spectrum laser, and selectively imaged using a dichroic filter set specific to 574nm wavelength emission (Semrock).

Calcium Influx

During stream acquisition, calcium ionophores Ionomycin and A23187 were used to induce calcium influx in vitro. Plated cells were cultured within 200ul of media just before imaging by TIRF-M. During imaging, either 200ul of .5uM Ionomycin was added

to yield a .25uM treatment, or 200ul of 5uM A23187 to yield a 2.5uM treatment. Starting concentrations for each of these ionophores were determined by review of literature[73,81], and were further optimized by titrations to reach ideal effect while maintaining cell viability.

CHAPTER FOUR

ALPHA SYNUCLEIN INDUCES CATHEPSIN B DISPERSION

INTRODUCTION

Lysosomal dysfunction has been implicated as the physiological mechanism behind numerous diseases and is known to negatively impact mitochondrial function in addition to other essential functions of the cell, leading to cell damage and loss[83,84]. Further, the majority of diseases related to lysosomal dysfunction are a direct result of deficiencies in enzymes within the lysosomal lumen, resulting in toxicity and cell death.[84] Previous findings support the notion that synucleinopathies may lead to the same lysosomal enzyme deficiencies through induced lysosomal membrane damage[7]. If this is the case, aberrant forms of α-syn may induce the release of active proteases into the cytosol, a process that could be a direct mechanistic explanation of α-syn toxicity. A strong tool for the verification of this process in this study has been be the use of known lysosomal disruptor, LLOMe, which has been shown to induce cathepsin-dependent cell death as a well characterized parallel to α-syn induced lysosomal rupture and cell death[85].

Previous studies have indicated potential cellular repercussions of vesicle rupture and subsequent release of active cathepsins, but there is currently no direct evidence of cathepsin release in models of PD. We aim to confirm this occurrence in order to corroborate our previous findings of lysosomal rupture induced by α-syn, and also to further implicate the tBid apoptosis pathway in PD pathology. We hypothesize that samples treated with α-syn will have significantly increased lysosomal vesicle rupture events, measured by both increased galectin 3 puncta and dissipation of signal from IF labeled

lysosomal proteases (**Figure #3**). Therefore, we expect to measure decreased Cathepsin B puncta in samples treated with α-syn aggregates compared to untreated samples.

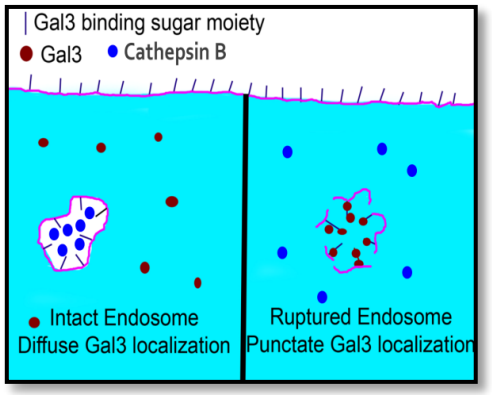

Figure 3. Model of cathepsin B dispersion within chGal3 expressing cells.

EXPERIMENTAL DESIGN

SH-SY5Y neuroblastoma cells expressing mCherry-Galectin 3 were plated onto Fibronectin coated coverslips at a density of 25,000 cells/ml within a 24-well plate and allowed to adhere overnight. For plating, cells were initially separated into three groups: untreated, α-syn treated, and a negative control for cathepsin B which involved secondary antibody staining only. In later trials, a positive control for vesicle rupture was added as a fourth sample group, which consisted of 10mM LLOMe treatment. The following day, conditioned DMEM was aspirated and replaced with either 500ul of fresh DMEM for nontreated control and LLOMe samples, or 500ul fresh DMEM containing 3ug/mL α-syn for treated samples and secondary only control samples. After 24 hours of α-syn treatment, samples were fixed and stained for cathepsin B. Samples were then mounted to slides with Fluoromount^{TM} Aqueous Mounting Medium (Sigma-Aldrich), imaged using fluorescence deconvolution microscopy, and analyzed for prevalence of cathepsin B puncta. A secondary only control was included to confirm specificity of primary antibodies.

To determine the legitimacy of cathepsin B staining, a simultaneous IF stain for mouse anti-EEA1 and mouse anti-LAMP-2, labeled with subsequent incubation with 488-conjugated anti-mouse secondary antibody, was performed in conjunction with cathepsin B staining to confirm cathepsin B localization to all relevant vesicular compartments.

RESULTS

Early experiments in this series showed promising results in favor of α-syn induced cathepsin B dispersion. When chGal3 expressing SH-SY5Y cells were treated with 3ug/ml α-syn aggregates, there was an extremely significant decrease in the number of detected cathepsin B puncta compared to untreated controls in select trials (**Figure #4-i & iv**). Replicate experiments were carried out in the pursuit of additional evidence to strengthen our conclusions, and to overcome initial issues with chGal3 signal loss during IF staining. In later trials, the duration of the cell fixation protocol was increased from 5 to 20 minutes, which gave rise to successful retention of chGal3 rupture signal through IF staining (**Figure #4-ii)**. However, later trials failed to produce significant dispersion of cathepsin B staining, even after multiple replicates were conducted. In an attempt to achieve unequivocal cathepsin B dispersion, cells were treated with LLOMe at a generous 10 mM concentration. These positive control samples displayed clear and extensive rupture (**Figure #4-iii**), yet failed to produce differences in the prevalence of cathepsin B puncta per cell compared to untreated samples, even after several trials (**Figure #4-v**). Due to our interest in cytososolic cathepsin B dispersion as an effector of cell viability, we decided to alter our analysis to exclude irrelevant nuclear and extracellular cathepsin B signal through the use of image masking in the Imaris software package (Bitplane) with the hope that it may unveil a larger margin of difference in

cytosolic cathepsin B puncta between treated and untreated samples (**Figure #5**). Although image masking did appear to have this effect to some extent, even these trials failed to achieve significance (**Figure #4-vi**). In a final attempt to determine the fault in our experimental design, cells were simultaneously stained for EEA1 and LAMP2 in the 488nm emission channel, in addition to cathepsin B in the 576nm emission channel, at which point it became clear that our cathepsin B stain with different antibodies was not colocalizing with known markers of protease containing vesicles, and therefore must be producing a non-specific signal (**Figure #6**).

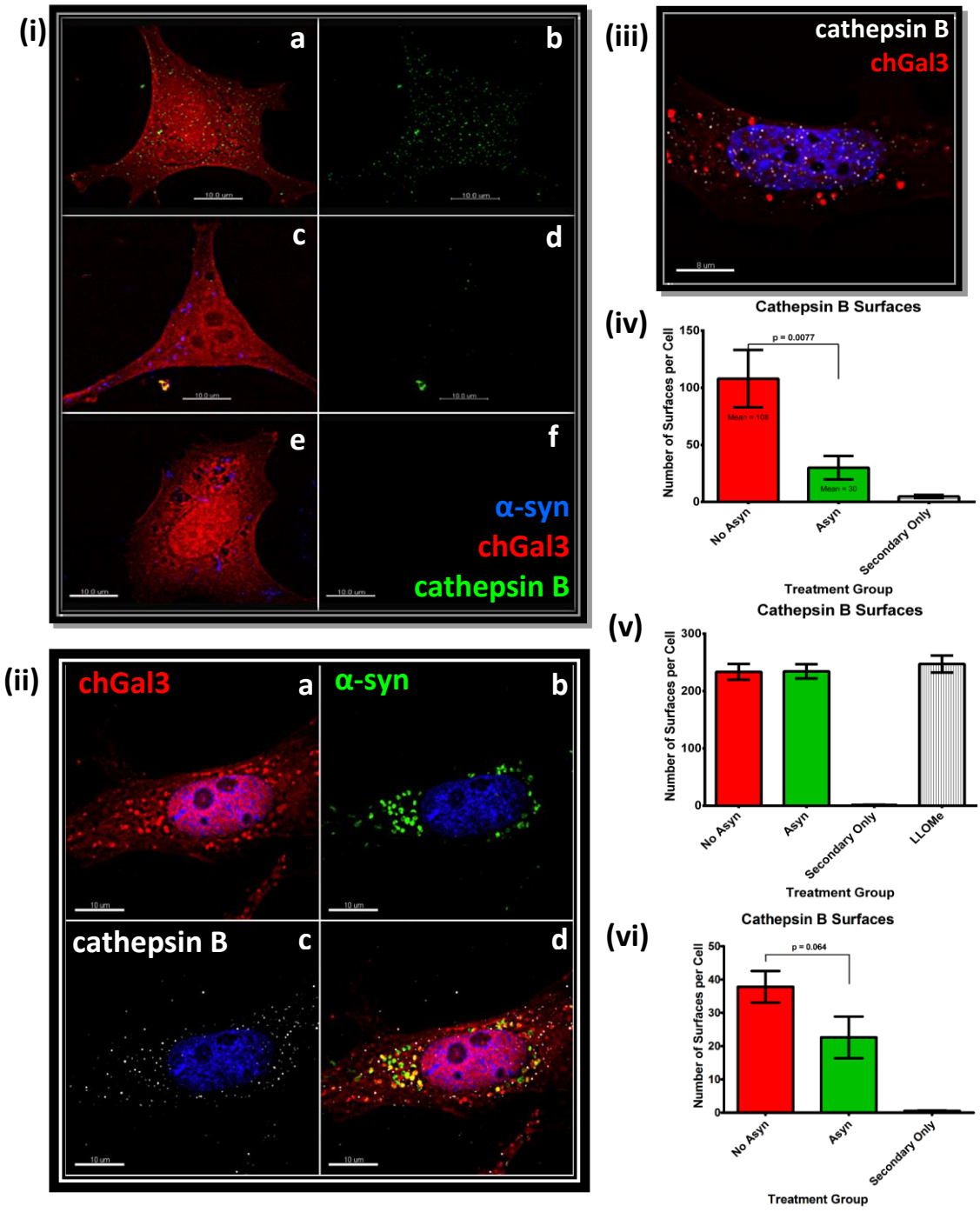

Figure 4. Cathepsin B Dispersion Results (i) chGal3 SH-SY5Y cells (a) Untreated for 24 hours, fixed, and IF stained for Cathepsin B. (c) Treated with 3ug/ml of α-syn for 24 hours, fixed and IF stained for Cathepsin B. (e) Repeat of (c) without primary antibody staining. Primary staining done with 0.5ug/ml of polyclonal rabbit anti-cathepsin B (Santa Cruz), and secondary staining with 1:500 dog anti-rabbit 676. Panels (b), (d), and (f) are duplicate images of the preceding column with only Cathepsin B displayed. **(ii)** Successful retention of chGal3 puncta, displaying rupture induced by α-syn in independent channels for chGal3 (a), α-syn (b), cathepsin B (c), and merged (d). **(iii)** LLOMe treated samples induce lysosomal rupture apparent by chGal3 puncta formation. **(iv)** Quantification of Cathepsin B surfaces between treatment groups for a single trial (15 images per group). **(v)** Common results which failed to achieve significance, even with 10 mM LLOMe treatment. **(vi)** Post masking results from panel **(v)** demonstrate improved significance by masking in select instances. Images are pseudo-colored for optimal visualization of specific effects.

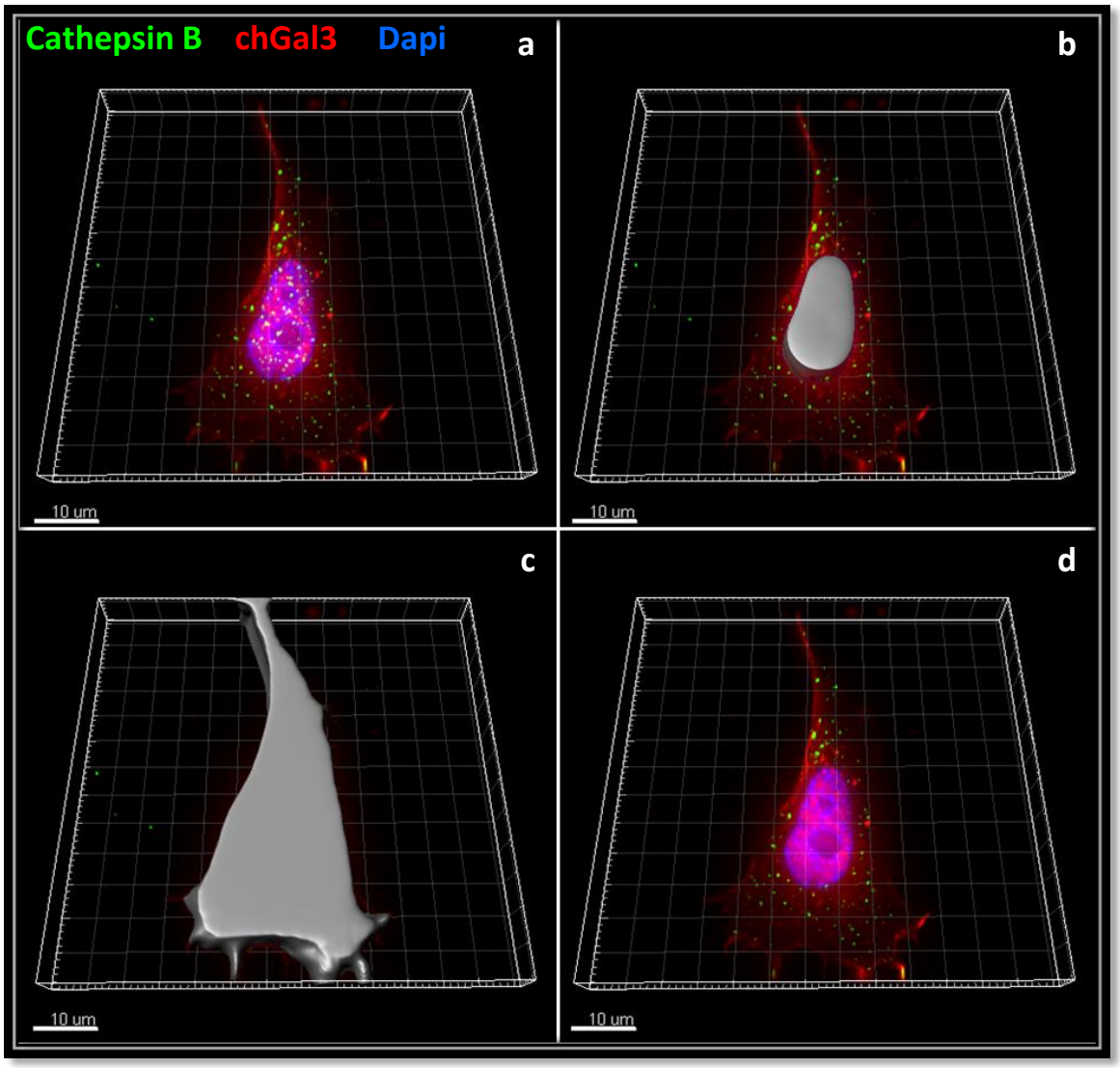

Figure 5. Demonstration of the cell masking process for exclusion of nuclear and extracellular cathepsin B puncta. Panel A represents raw images before masking. Nuclear puncta were excluded by setting cathepsin B staining within DAPI masks to a fluorescence level of zero (B). Extracellular cathepsin B staining was excluded by setting puncta outside of chGal3 whole-cell masks equal to zero (C). Post masking images (D) were then analyzed for total cytosolic cathepsin B puncta using the high-throughput Batch tool of Imaris (Bitplane).

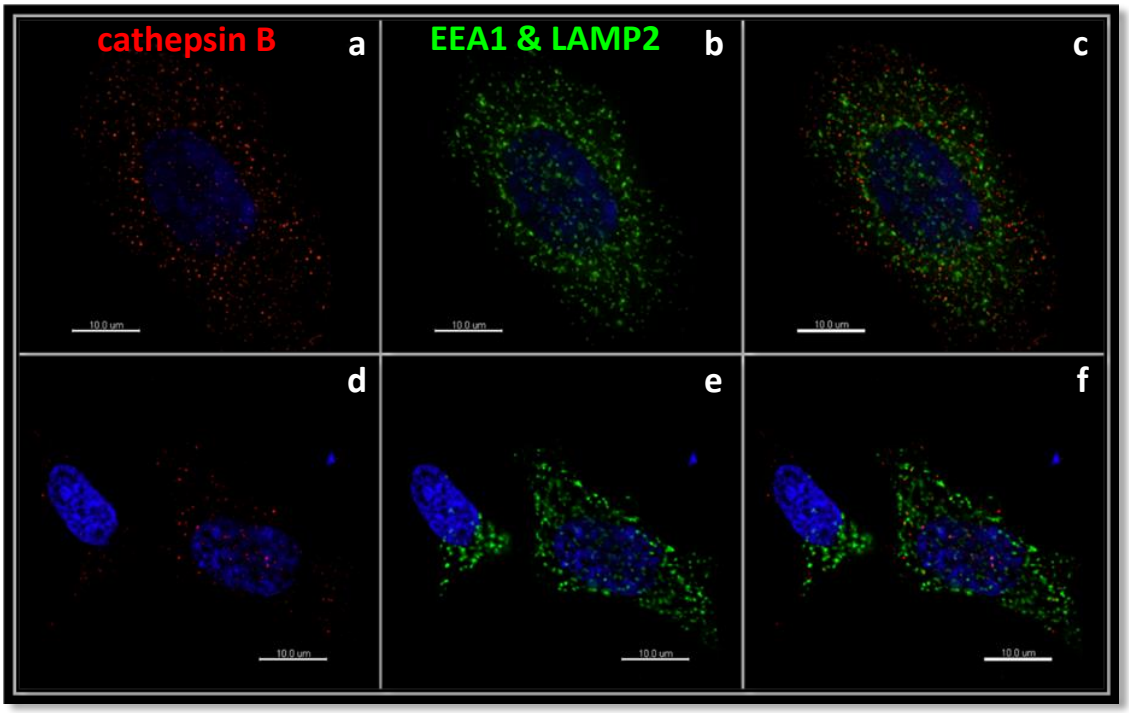

Figure 6. Confirmation of non-specific anti-cathepsin B binding. Wild type SH-SY5Y cells were plated onto Fibronectin coated coverslips 24 hours prior to fixation. Cells were then IF stained with one of two polyclonal, rabbit anti-Cathepsin B antibodies (Abcam at 1ug/ml in panels (a), (b) and (c), or Santa Cruz at 0.5ug/ml in panels (d), (e) and (f)). All vesicles that should contain either pro-cathepsin B or mature cathepsin-B, including early endosomes, primary lysosomes, and secondary lysosomes (endocytic and autophagic), have been immunofluorescently labeled by simultaneous IF staining with mouse anti-EEA1 and mouse anti-LAMP2 primary antibodies followed by anti-mouse 488 secondary staining. Images were then analyzed for colocalization. Images in each row are the same field. The far left column displays Cathepsin B and DAPI. The central column displays EEA1/LAMP2 and DAPI. The far right column displays merged images.

DISCUSSION

Due to the confirmed intraluminal localization of cathepsin B to acidified vesicles under normal conditions, cathepsin B signal from IF staining should parallel that of the live cell Lysotracker dye which serves as a marker of acidic compartments[86,87]. Contrary to our expectations, however, the resulting puncta from IF staining of cathepsin B was far more abundant, had a much smaller than expected size distribution, and was present both extracellularly and within the nuclei of stained neuronal cells. Additionally, the results from the preliminary experiments of this study indicated a strikingly significant decrease in cathepsin B puncta with treatment of α-syn aggregates, despite there being essentially no measurable rupture events (chGal3 puncta) to explain the cathepsin B dispersion (**Figure #4-i**). Although secondary only controls were successful (**Figure #4-i),** these uncharacteristic staining patterns prompted further investigation into the binding specificity of the anti cathepsin B primary antibodies. Several trials of the experiment were repeated adjusting cell fix duration, antibody incubation time, α-synuclein species, and data analysis (masking), yet repeat experiments continuously failed to achieve significance. In later trials, chGal3 puncta was successfully retained through the IF protocol, most likely due to an increase in cell fixation from 5 to 20 minutes, however, overall results of cathepsin B dispersion as a result of α-syn treatment never achieved significance in triplicate.

As a positive control for the lysosomal rupture that α-syn aggregates are capable of inducing, samples were treated with the peptide drug LLOMe. Initially, samples were treated with 1mM LLOMe based on previously published work[45], but treatment concentration was eventually adjusted to 10mM after titration experiments were conducted

to elicit an appropriate effect in our specific cell line. Even the drastically high levels of rupture measured in the LLOMe treated samples resulted in no measurable difference in cathepsin B puncta, indicating no form of dispersion. At this point in the study, the only factor left invalidated was the primary anti-cathepsin B antibodies, which became highly suspect for nonspecific binding. To determine conclusively whether the cathepsin B staining in this study was legitimate, a simultaneous IF stain for mouse EEA1, LAMP-2, and cathepsin B was performed. This control served as final confirmation that the IF signal of each of the anti-cathepsin B antibodies used was entirely non-specific and did not colocalize with the previously characterized EEA1 or LAMP2 antibody stains as expected. These results confirmed that the preliminary measured effect cannot be explained by treatment with α-syn, making this aim of our study inconclusive. Due to the certain detrimental effects that cathepsin B dispersion could cause within neuronal populations (**Figure #7)**, future experiments will be conducted to accurately investigate the effect of α-syn treatment on lysosomal protease localization.

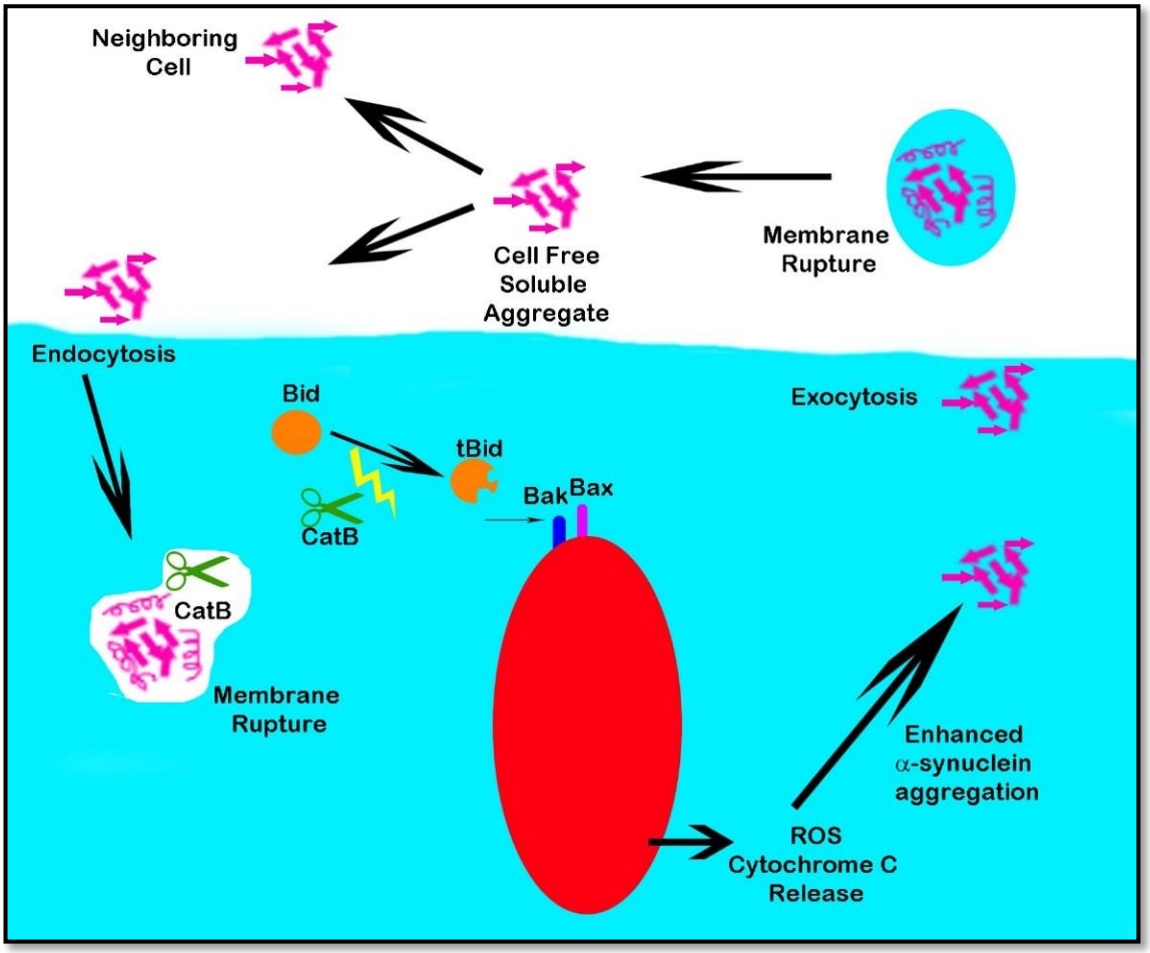

Figure 7. **Full model of cathepsin B dependent cell death** as a down-stream effect of α-syn induced rupture.

`

CHAPTER FIVE

POST-RUPTURE LYSOSOMAL FUNCTION

INTRODUCTION

Understanding the fate of lysosomes after α-syn-induced rupture will be critical to understanding intracellular trafficking and propagation of α-syn in synucleinopathies. If we can identify the prevalence of various post-rupture lysosomal populations, we can begin to confirm details of α-syn toxicity and form more accurate hypotheses about the mechanistic details of pathogenic α-syn aggregation and propagation. The primary purpose of this study was to determine if lysosomes are completely destroyed by rupture events. If lysosomes are completely and permanently ruptured by α-syn aggregates, this would result in a complete loss of functional degradation, release of lysosomal contents, and subsequent contribution of exogenous α-syn to the formation of cytosolic inclusions. Each of these events can contribute to increased strain on remaining cellular degradative pathways over time, and can directly promote cell death through activation of previously mentioned necrotic or apoptotic pathways. Alternatively, lysosomes may be minimally permeabilized in some cases, causing functional loss due to proton leakage without complete release of contained α-syn aggregates. If this is the case, these non-functional lysosomes containing α-syn may become targets for macroautophagy, resulting in their engulfment to form MVB-like structures and subsequent, non-classical release of α-syn by fusion with the plasma membrane to secrete exosome-like vesicles of lysosomal origin. Conversely, perhaps a significant number of lysosomes are able to reseal following α-syn induced rupture, thereby regaining function and maintaining involvement in both degradation of

accumulating α-syn aggregates. We hypothesized that the majority of lysosomes would rupture to the extent that they permanently lose degradative capacity, indicated by low prevalence of lysosomes (Lysotracker positive) that are also positive for the chGal3 rupture marker.

EXPERIMENTAL DESIGN

The same SH-SY5Y chGal3 cells were plated in 1 mL of DMEM at a density of 50,000 cells/ml onto Fibronectin coated live-cell Delta T dishes and allowed to adhere overnight. The following day, the conditioned media was replaced with 1 mL of fresh DMEM containing 3 ug/ml of aggregated and labeled α-syn. In control dishes, the same media changes were performed using media lacking α-syn. After 24 hours of treatment with α-syn aggregates, dishes washed with fresh DMEM and sequentially treated with 25nM Lysotracker dye in colorless DMEM for 20 minutes, followed by final replacement of media with standard colorless DMEM immediately before imaging. Images were then collected using wide field deconvolution microscopy, and analyzed for colocalization on the Imaris software package by Bitplane. Control samples undergoing parallel media changes, but lacking α-syn treatment, were used to validate the chGal3 rupture system in this context.

Colocalization Analysis

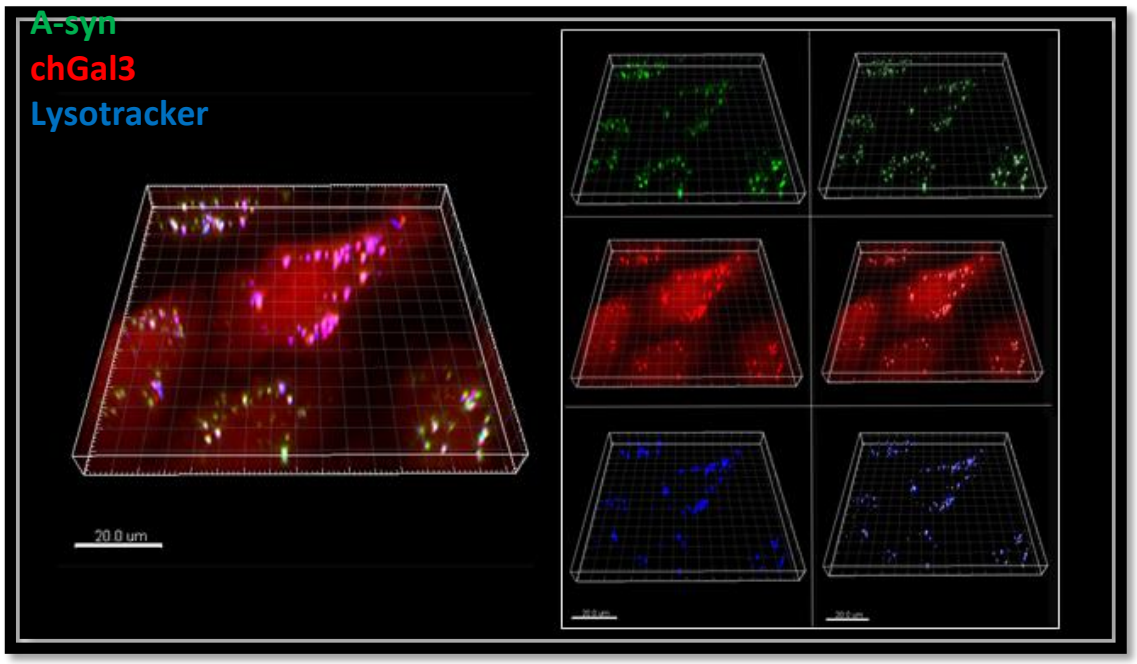

Figure 8. Three dimensional fluorescent images of the colocalization analysis process in SH-SY5Y cells. The far left image is a composite of all three channels. Middle column displays the indicated, individual channels. The far right column displays surface algorithm applied to detect puncta characteristics in each independent channel.

RESULTS

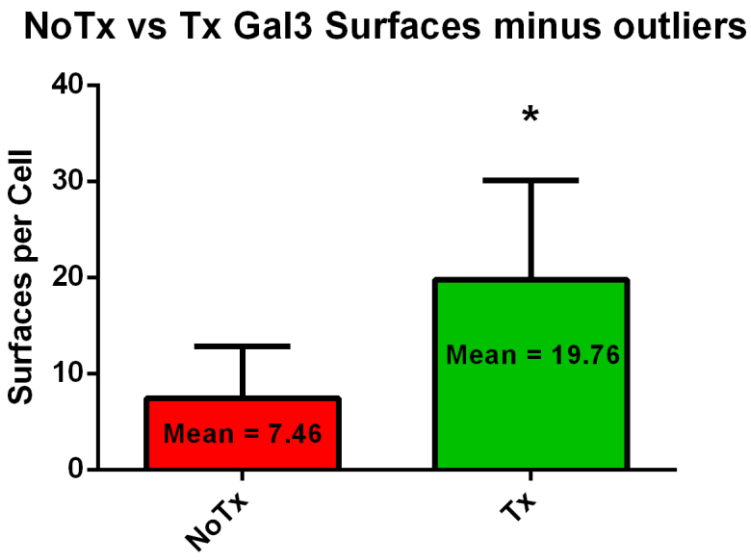

Figure 9. The effect of α-syn treatment on chGal3 labeled rupture events.

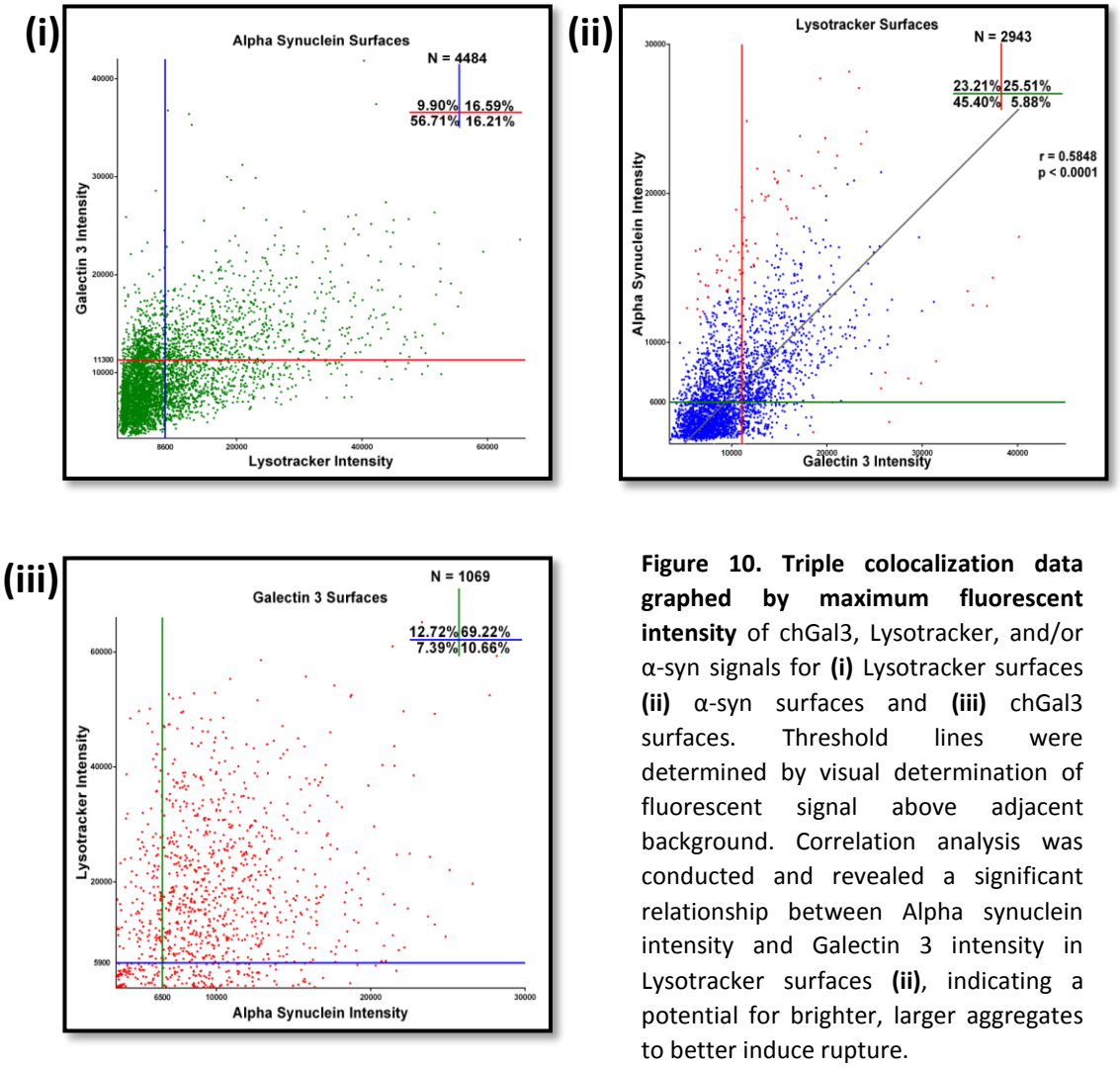

Figure 10. Triple colocalization data graphed by maximum fluorescent intensity of chGal3, Lysotracker, and/or α-syn signals for **(i)** Lysotracker surfaces **(ii)** α-syn surfaces and **(iii)** chGal3 surfaces. Threshold lines were determined by visual determination of fluorescent signal above adjacent background. Correlation analysis was conducted and revealed a significant relationship between Alpha synuclein intensity and Galectin 3 intensity in Lysotracker surfaces **(ii)**, indicating a potential for brighter, larger aggregates to better induce rupture.

The results of this experiment expand our current understanding of vesicle rupture by revealing various existing vesicle populations as exogenous α-syn is processed by the cell. The colocalization data above are displayed much like data acquired by FACS, although data points represent individual vesicles rather than cells (**Figure #10**).

Alpha synuclein surfaces (**Figure #11**) represent all surfaces built around α-syn puncta. Of these surfaces, the largest portion are positive only for α-syn (mean = 54.3%). This population may represent α-syn bound to the extracellular surface, contained within early endosomes that have yet to acidify, or α-syn that has ruptured and escaped vesicles to exist independently in the cytosol. Conversely, the smallest population of α-syn surfaces were double positive for α-syn and chGal3 (α-syn^{+}/chGal3^{+}). This type of colocalization between chGal3 and α-syn is most likely to occur through a mutual interaction with the vesicle membrane, meaning that the α-syn^{+}/chGal3^{+} population represents ruptured vesicles that have remained bound to α-syn (mean = 8.6%)[46,50]. Surfaces built around α-syn puncta that were positive for Lysotracker were fairly prevalent as well (15.7%), supporting previous findings that α-syn aggregates are taken up through the endocytic pathway where their host endosome can fuse with primary lysosomes[79]. Most notably, the presence of triple positive population of α-syn surfaces (21.2%) suggests that ruptured α-syn^{+}/chGal3^{+} vesicles are likely to be sequestered within acidified compartments through unconfirmed mechanisms.

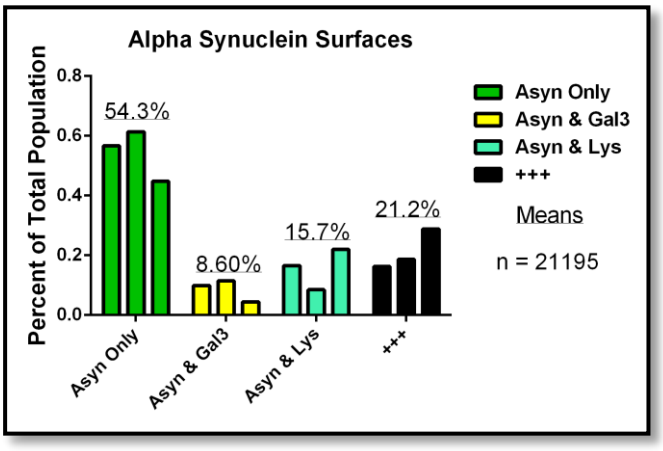

Figure 11. Triplicate means of colocalization populations within α-syn surfaces.

Lysotracker surfaces (**Figure #12**), on the other hand, represent all intact, low pH organelles, which may include a small population of late endosomes and autophagosomes, but mainly encompasses primary and secondary lysosomes (ThermoFisher). Surprisingly, the most prevalent population of Lysotracker surfaces were triple positive (44.1%), in contradiction to our predictions that this population would not exist. Similar to the populations from other surfaces, the two double positive populations were the least abundant. The population of Lysotracker and α-syn positive surfaces is measured a second time here in the context of Lysotracker surfaces rather than α-syn surfaces, and again, represents pre-rupture endocytic lysosomes containing α-syn aggregates (19.8%). Vesicles double positive for Lysotracker and chGal3 may represent various events. Maybe they arise as a result of autophagic uptake of chGal3 positive debris from previous lysosomal rupture. Perhaps these Lysotracker and chGal3 positive vesicles occur due to lysosomal reseal after rupture, followed by successful degradation of the offending α-syn aggregate. However, this population is the least abundant (6.92%), and is therefore less likely to be a main outcome in α-syn intracellular trafficking. More certainly, Lysotracker only surfaces (29.1%) are likely to represent the pool of primary lysosomes prior to formation of secondary lysosomes through fusion with either endosomes or autophagosomes. Interestingly, the population distribution of lysosomes from the pool of Lysotracker only vesicles appears to vary inversely with the population of triple positive lysosomes between trials (**Figure #12**).

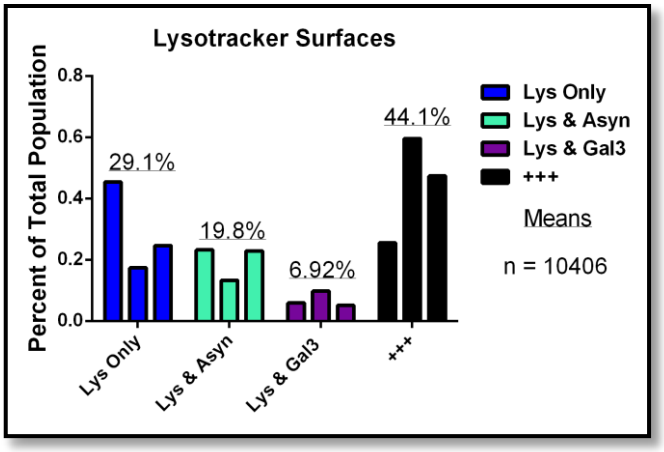

Figure 12. Triplicate means of colocalization populations within Lysotracker surfaces.

Galectin 3 surfaces (**Figure #13**) mainly represent lysosomal rupture events, and a small portion of early endosomal rupture based on previous results[7]. Of the cumulative 6,190 rupture events measured between trials (galectin 3 surfaces), a surprising average of 73.6% of rupture events were also positive for Lysotracker and α-syn. An average of 20.05% of rupture events were negative for Lysotracker, indicating that a significant population of lysosomes at this time point experience rupture which disrupts the low pH environment of the lysosome and causes dispersion of the Lysotracker dye. In line with common observation from previous surface analysis, the population of Lysotracker/chGal3 positive vesicles are the least abundant (6.36%). Galectin-3 puncta also underwent additional investigation to determine prevalence between untreated and α-syn treated samples. It is worth noting that the chGal3 assay system is not perfect, and does produce background signal from spontaneous rupture to a small extent in untreated samples. However, the results from this analysis demonstrate a substantial increase in chGal3

labeled rupture induced by α-syn treatment, demonstrating the validity of the assay (**Figure #9**).

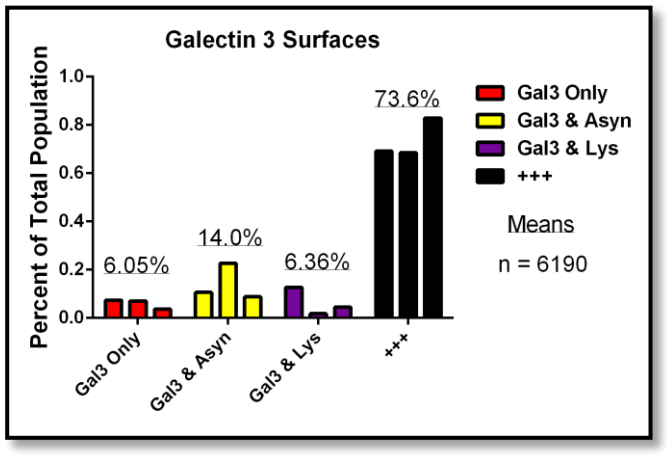

Figure 13. Triplicate means of colocalization populations within chGal3 surfaces.

These results most importantly raise questions about the population of triple positive puncta abundantly present in each of the surface analyses. What do they represent, and how are they formed? Could triple positive puncta indicate a potential for lysosomes to reseal after rupture, or are ruptured α-syn^{+}/chGal3^{+} lysosomes rendered non-functional and therefore simply targeted for macroautophagy and sequestered back inside of independent acidified autolysosomes?

In order to more accurately address this key question, volumes of α-syn, chGal3, and Lysotracker surfaces were analyzed between these different populations. This analysis was based on the idea that resealed lysosomes would maintain relatively constant volumes within these two surfaces, while triple positive puncta formed through macroautophagic uptake of previously ruptured vesicles would likely vary more widely in volume. Volume analysis reveals fascinating evidence that the triple positive puncta contain far larger volumes of α-syn aggregates and larger volumes of Lysotracker dye compared to single

positive puncta of either marker (**Figure #14-i & ii**). To supplement this data, maximum intensity between colocalization populations was also analyzed (**Figure #14-iii**).

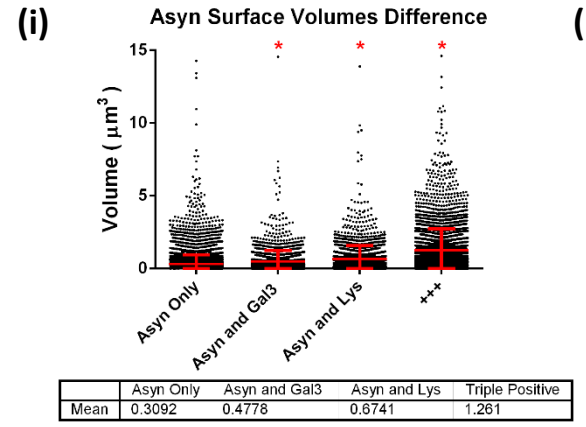

	Asyn Only	Asyn and Gal3	Asyn and Lys	Triple Positive
Mean	0.3092	0.4778	0.6741	1.261

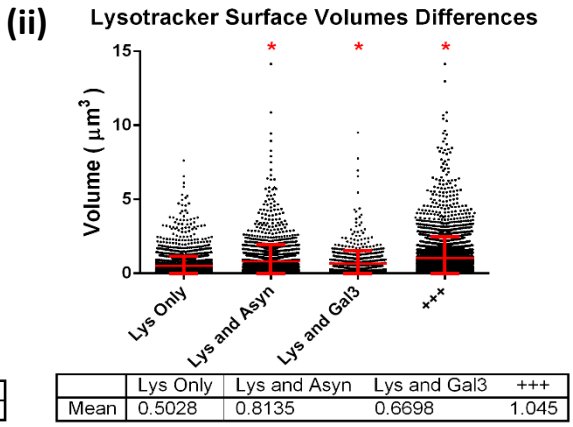

	Lys Only	Lys and Asyn	Lys and Gal3	+++
Mean	0.5028	0.8135	0.6698	1.045

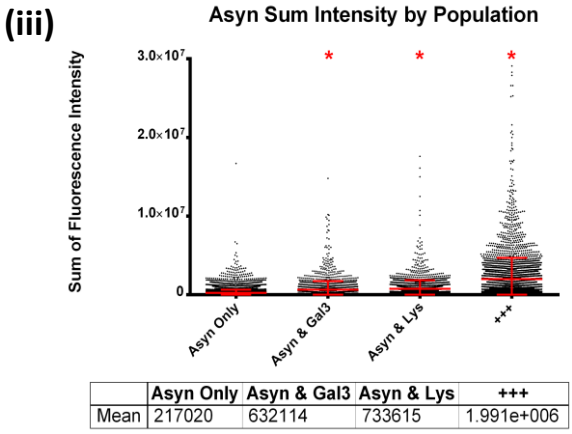

	Asyn Only	Asyn & Gal3	Asyn & Lys	+++
Mean	217020	632114	733615	1.991e+006

Figure 14. Volume differences between four colocalization populations in α-syn surfaces **(i)** and Lysotracker surfaces **(ii),** and maximum fluorescence intensity differences between the four colocalization populations in α-syn surfaces **(iii).** All graphs include results from triplicate experiments.

DISCUSSION

Based on the results of this study and previously published findings, the following vesicle outcome map has been generated to predict intermediate phases of intracellular α-syn trafficking from uptake to release.

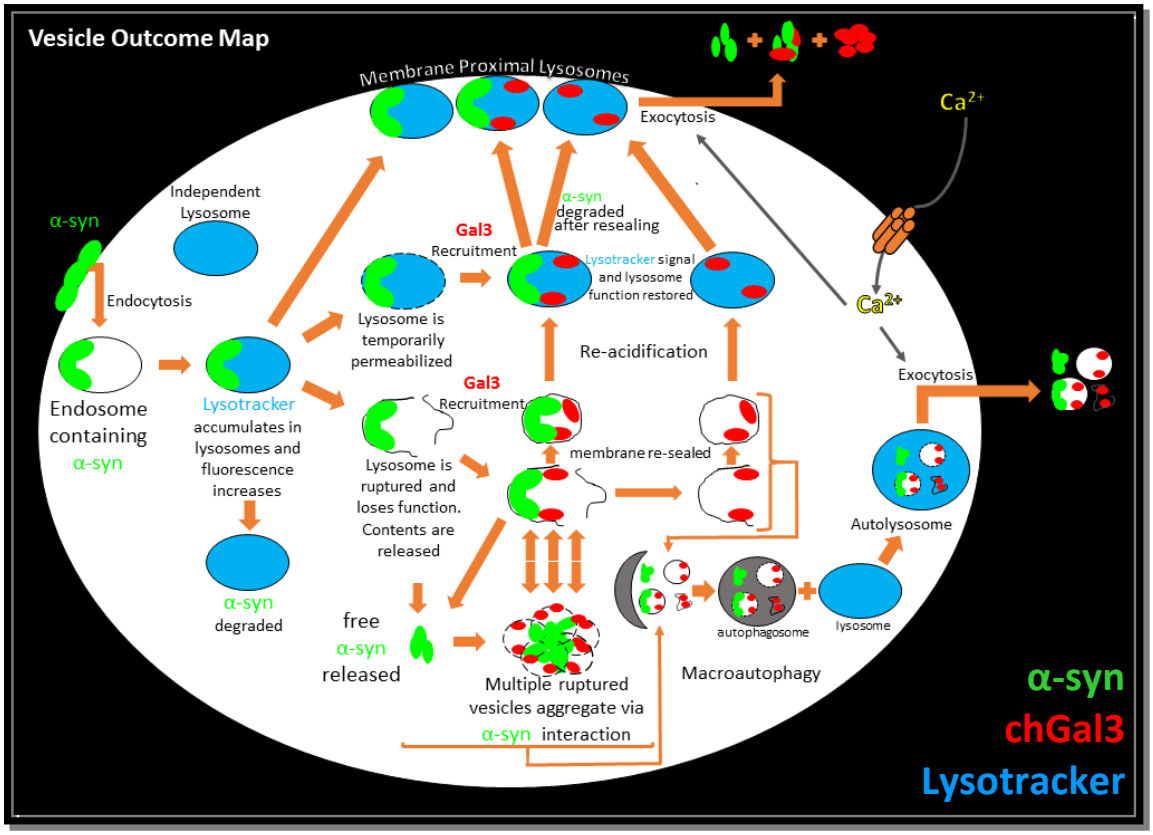

Figure 15. Vesicle outcome map depicting potential pathways for the intracellular trafficking of α-syn aggregates in a whole-cell context. Initial endocytosis is depicted on the left side. As α-syn progresses through the endocytic pathway, the host vesicle acidifies, sequestering acidophilic Lysotracker dye to become Lysotracker positive. Double positive lysosomes containing α-syn may then successfully degrade α-syn, or rupture to recruit chGal3. Lysosomal rupture may occur transiently, allowing lysosomes to reseal (top path), or may result in complete disruption of the lysosomal membrane and loss of Lysotracker signal (bottom path). Intact, post-rupture lysosomes may continue to function, or may exist as acidic, Lysotracker positive, yet non-functional vesicles devoid of necessary proteases, in which case they may undergo lysosomal exocytosis to deposit accumulated contents (top). If lysosomes are fully ruptured, however, they may become targets for macroautophagy to end up as triple positive species to undergo continued degradation of accumulating α-syn, or simply undergo lysosomal exocytosis to release apparent 'exosome-like' structures from the cell (far right). Lysosomal exocytosis is a calcium dependent process.

The path of exogenous α-syn aggregates as they are processed by the cell has become considerably more clear based on the results of this study. Initially, α-syn aggregates can be seen as independently fluorescent puncta near PM, likely contained within early endosomes (Figure). This early-entry population of α-syn is likely to account for a large majority of 'α-syn only' positive surfaces (**Figure #11**). The exact mechanisms of uptake remain to be elucidated, but our detection of double positive α-syn and Lysotracker vesicles serves as substantial evidence, in agreement with previous findings, that α-syn is taken up through the endocytic pathway to be contained within endocytic lysosomes[79].

Once the α-syn aggregates are internalized, the mechanism in which they gain access to the cytosol has been widely debated[4]. Although our data does not specifically highlight temporal aspects of intracellular α-syn trafficking, it does strongly corroborate our previous findings and hypothesis that vesicle rupture is the mechanism of cytosolic entry for exogenous α-syn aggregates[7]. If rupture does occur later in the endocytic pathway at the stage of endocytic lysosomes, as per our previous findings[7], then it can be said that the chGal3 surfaces predominantly represent ruptured lysosomes. Under this assumption, our chGal3 data indicates that at least 20.05% of rupture events induced by α-syn cause dissipation of Lysotracker signal, indicating severe disruption of the lysosomal membrane leading to the dissipation of luminal contents. In each of these cases, α-syn is likely to be exposed in the cytosol with the potential to interact with other exogenous aggregates and act as a template for misfolding of endogenous α-syn, ultimately explaining the ability of exogenous aggregates to contribute to the development of toxic LB and LN structures[3,65,66]. Furthermore, the subset of rupture

events that are positive for chGal3 alone (6.05%) represent potential for complete release of free α-syn aggregates from ruptured vesicles into the cytosol to induce the same, unhindered nucleation effect.

In fact, it is possible that a much larger population of rupture events causes complete destruction of lysosomes, depending on the origin of triple positive puncta. There are two possible outcomes for ruptured lysosomes that could give rise to the triple positive vesicles observed in this study. First, lysosomes may remain independently functional after transient permeabilization, retention of α-syn aggregates, and recruitment of chGal3. However, if this were the case, the overall volume of triple positive vesicles would be likely remain constant, making primary lysosomes (Lysotracker only) the same size as triple positive vesicles. Based on our volume analysis of both α-syn and Lysotracker surfaces, we can confidently say that this is not always the case. A significant population of triple positive puncta contain much larger volumes of α-syn aggregates than α-syn aggregates in pre-ruptured lysosomes (means = 1.261 μm^3 vs 0.3092 μm^3, respectively), with higher fluorescence intensities (**Figure #14-i & iii**). Additional analysis of Lysotracker surface volumes reveals the same pattern of increased volume for triple positive puncta compared to Lysotracker only, primary lysosomes (means = 1.045 μm^3 vs 0.5028 μm^3) (**Figure #14-ii**), reflecting the known volume differences between primary lysosomes and autolysosomes (lysosome volume range: up to 0.065 μm^3, autolysosome volume range: up to several μm^3)[88,89]. These results strongly suggest that triple positive vesicles can be formed by cumulative recruitment of ruptured $\alpha\text{-syn}^+/\text{chGal3}^+$ lysosomes to distinct intact lysosomes, which, through known mechanisms, could only be explained by macroautophagy. Uptake of these ruptured

lysosomes is also likely to be occurring at a rate which exceeds the degradative capacity of the autolysosomes, especially under these conditions of lysosomal dysfunction. This indicates that a significant portion of the triple positive puncta also include previous, fully ruptured lysosomes, meaning that the frequency of complete lysosomal destruction by α-syn is certainly larger than the mentioned 20.05%. Of course, this large scale occurrence of lysosomal destruction would have extremely detrimental effects on neuronal populations in vivo.

In support of our findings, the Yoshimori lab at the University of Osaka recently demonstrated the concept that damaged lysosomes can become targets for autophagy[45]. Evidence from their study suggests that lysosomal rupture induces upregulation in autophagy, allowing the clearance of ruptured lysosomes. However, in cells deficient of essential autophagic proteins, clearance of these ruptured lysosomes was fully attenuated[45]. These findings, in congruence with our own, lead us to the conclusion that the majority of ruptured lysosomes are not simply resealing after rupture, but instead are being taken up, and accumulating within distinct lysosomal compartments through macroautophagic mechanisms.

CHAPTER SIX

CALCIUM-DEPENDENT RELEASE OF α-SYNUCLEIN

INTRODUCTION

Thus far, this study has shed light on mechanisms of uptake and intracellular processing of exogenous α-syn aggregates, but has yet to address the mechanisms behind well documented α-syn release and intercellular propagation. If exogenous α-syn aggregates do progress through the cell, inducing lysosomal rupture, and eventually becoming secondarily sequestered within autolysosomes, then how can previous findings of α-syn release from cells be explained?

It has been determined that α-syn aggregates can be released from cells in a calcium dependent manner in apparent vesicular fractions that have been referred to as exosomes[81]. Beyond this, compelling evidence from multiple studies suggests that lysosomal exocytosis occurs in response to calcium influx, especially in response to the membrane damage[73,76]. We hypothesize that under conditions of drastic ALP dysfunction, as is the case during accumulation of aberrant α-syn, lysosomes will be unable to properly degrade α-syn aggregates, and will therefore accumulate α-syn aggregates that may be released to the extracellular space through mechanisms of calcium-induced lysosomal exocytosis. Understanding whether known mechanisms of lysosomal exocytosis contribute to the propagation of toxic forms of α-syn could reveal important drug targets for therapeutic intervention. If lysosomal exocytosis is a predominant form of α-syn propagation, selective inhibition of this process in cells containing aberrant forms of α-syn aggregates may become an avenue of further investigation.

EXPERIMENTAL DESIGN

ChGal3 expressing SH-SY5Y cells were plated onto Fibronectin coated borosilicate chamber slides and allowed to adhere overnight. To image lysosomes in this context, cells were treated with 200ul of 1 uM LysoSensor™ Green DND-189 (ThermoFisher) in DMEM for 30 minutes prior to imaging. As per product protocol, cells remained cultured in LysoSensor™ containing media during imaging. For visualization of α-syn release, DMEM containing 3ug/ml of DyLight™ 488 labeled α-syn aggregates was then added to each well of the chamber slides for 24 hour treatment period. After α-syn treatment, media will be replaced with 200ul of fresh DMEM in each well, and cells will be imaged by TIRF microscopy. During imaging, calcium ionophores (Ionomycin or Ca2+ Ionophore A23187) will be added within 200ul of DMEM to initiate calcium influx. Cellular response to calcium influx will be measured by appearance of labeled α-syn, lysosomes, and galectin3 puncta to the basal plasma membrane. Fluorescence intensity over time will then be evaluated to identify fusion events of either individual lysosomes or MVBs.

RESULTS

For this preliminary study, TIRF microscopy was only achieved within the 488nm fluorescence emission channel due to limitations of available live cell lysosomal dyes and compatible fluorescence microscopy filters. For this reason, rather than looking at α-syn aggregates and lysosomal markers simultaneously, we attempted to first confirm our ability to induce calcium-dependent lysosomal exocytosis as seen in Simon et al[73]. Rather than expressing fluorophore conjugated lysosomal antigens, we attempted to label lysosomes using the only available live cell lysosomal marker available in the channel in which we could appropriately image using TIRF, LysoSensor™ Green DND-189 (ThermoFisher). The LysoSensor stain was fairly successful for visualization of endogenous acidified compartments by epifluorescence (**Figure #17**), but unfortunately produced significant staining of the plasma membrane that prevented proper visualization of lysosomal compartments while imaging by TIRF (**Figure #18**).

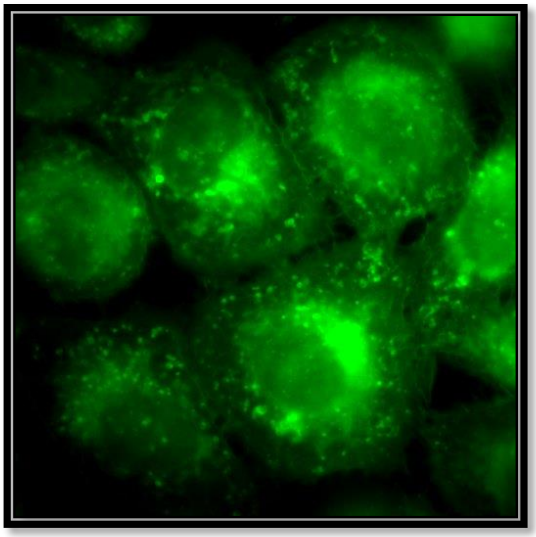

Figure 16. LysoSensor Staining visualized by epifluorescent excitation. Acidified vesicles can be distinguished

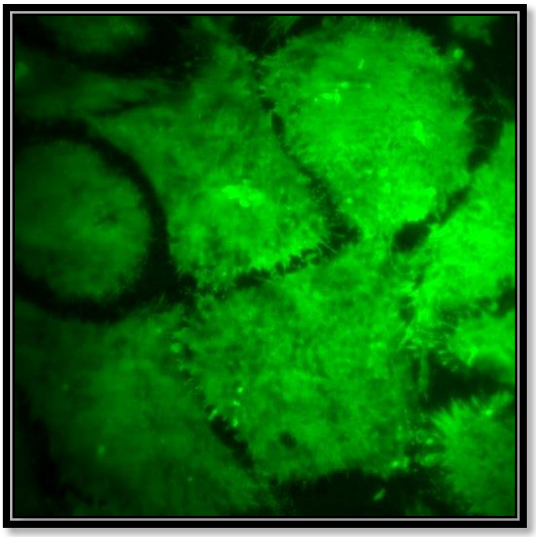

Figure 17. LysoSensor Staining visualized by TIRF excitation. Acidified vesicles cannot be distinguished through basal membrane

Despite this limitation of the LysoSensor™ stain, the possibility of direct visualization of calcium dependent α-syn release was still of key interest to us, especially as preliminary evidence to justify further study in this vein. During initial imaging of DyLight™ 488-labeled α-syn aggregates, a drastic increase in fluorescence intensity was measured at numerous points within the imaged field immediately following induced calcium influx (**Figure #19**). This may indicate calcium dependent migration of vesicular α-syn aggregates, likely contained within lysosomes and/or autolysosomes, to the plasma membrane. In some specific regions of interest, patterns of fluorescence dissipation that would be expected to occur during vesicular fusion events were measured (**Figure #20**).

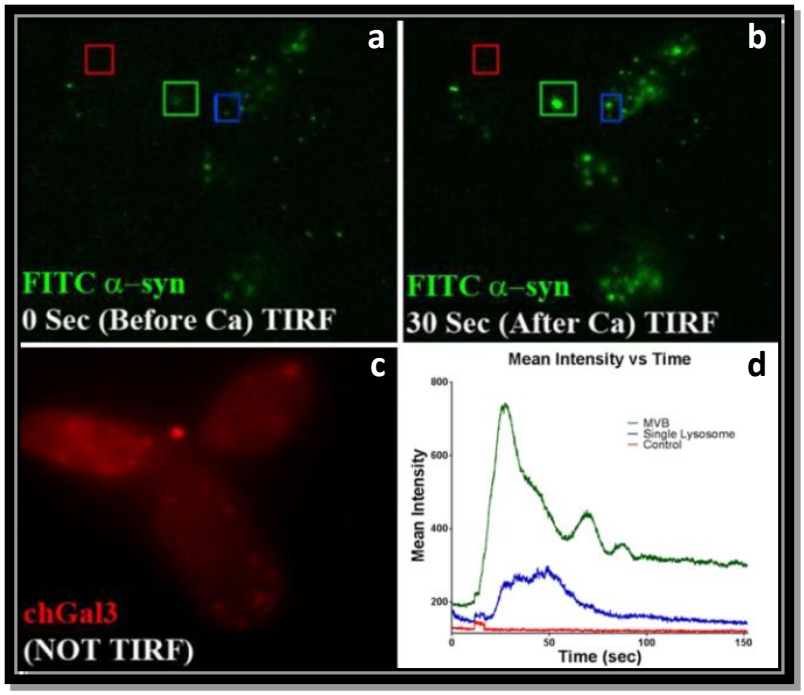

Figure 18. Demonstration of calcium-dependent α-syn release. Total internal reflection fluorescence image of chGal3 SH-SY5Y cells treated with α-syn aggregates for 24 hours at (a) time zero, before addition of calcium ionophore and (b) time 30 sec, after addition of calcium ionophore. Images in panels **a** and **b** are excited by 488 channel laser only. (c) Image of chGal3 localization with red laser excitation only. (d) Graph of mean fluorescence intensity over time

However, some puncta are much larger, brighter, and appear to remain more highly fluorescent over time, as indicated in **Figure #19** by the green box and corresponding fluorescence intensity graph. We suspect that this type of change in fluorescence over time is indicative of a MVB-like structure, likely an autolysosome containing α-syn and debris from previously ruptured vesicles, fusing with the PM to release both soluble and vesicular fractions. The majority of α-syn puncta that migrate to the PM in response to calcium influx appear to do so transiently. An example of this is depicted by the blue box and corresponding fluorescence intensity graph in **Figure #19**, where the punctate α-syn approaches the membrane and quickly returns to baseline intensity. This could indicate fusion of individual lysosomes to the PM, allowing release of primarily soluble contents into the extracellular space, resulting in a decrease of fluorescence intensity back to baseline.

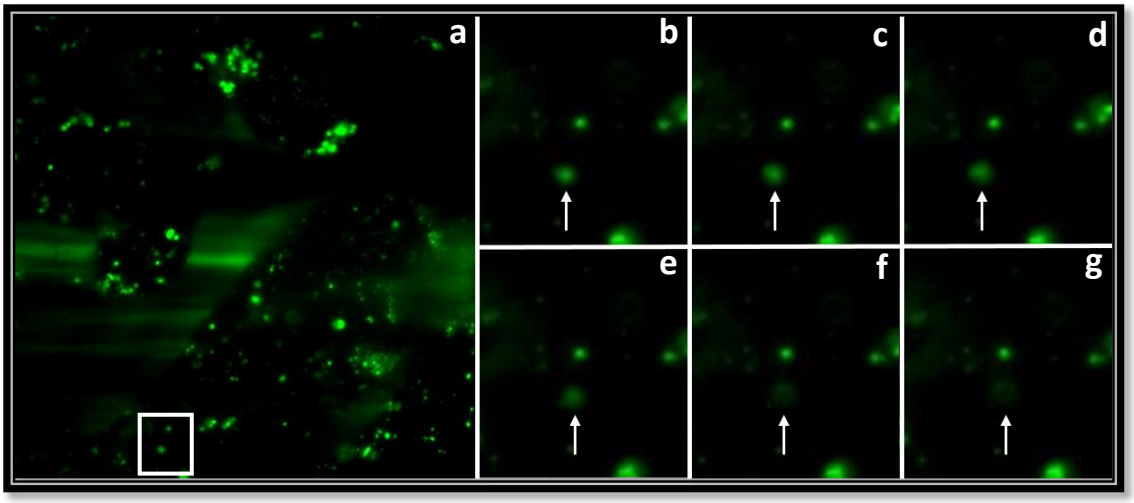

Figure 19. Potential release of α-syn by lysosomal exocytosis. (a) Full imaging field taken by TIRF-M. Multiple SH-SY5Y cells can be seen containing 488-labeled α-syn aggregates. (b-g) Enlarged region of interest from panel (a) displaying a potential fusion event in 1 second intervals after calcium influx.

DISCUSSION

Although the results of this preliminary study parallel those of lysosomal exocytosis in Simon et al[73], our findings were less profound. Based on the abundant localization of α-syn aggregates to lysosomal compartments demonstrated in this study and previously published studies[79], in conjunction with the abundant lysosomal exocytosis reported in Simon et al, we expected to visualize substantial release of α-syn aggregates in response to induced calcium influx. However, apparent fusion events were exceedingly rare. Our results raise questions about the factors that may influence cellular capacity for lysosomal exocytosis between different cell types.

Factors that may influence lysosomal exocytosis

It has been strongly established that vesicles equipped with SNARE complex proteins that are capable of calcium-dependent exocytosis exist in distinct pools localized to different cellular regions. So called 'fast' phase exocytosis occurs through the fusion of of vesicles proximal to inner leaflet of the plasma membrane that are docked and primed for fusion, awaiting calcium influx for final initiation of exocytosis[90]. More recently it has been demonstrated that lysosomes localize to distinct cellular regions much like secretory vesicles, with membrane proximal lysosomes being most capable of fast phase calcium-dependent exocytosis[73,91]. However, vesicles destined for exocytosis must first be recruited to the membrane from intracellular pools, the driving force for which is kinesin and myosin motor activity along microtubules and actin respectively[90]. However, efficient trafficking of lysosomes to the membrane for exocytosis is dependent on multiple factors, including cortical actin, calcium channel expression, cholesterol, and clatherin adaptor proteins essential for SNARE protein targeting[78]. These factors influencing lysosomal exocytosis

are likely to vary in function and prevalence between cell types, making it feasible that studies exhibiting efficient calcium dependent exocytosis in various non-neuronal cell types may not translate directly to the neuronal cell lines used in this study. Perhaps the use of primary dopaminergic neurons from the SNpc, which express specific $Ca_v1.3$ calcium channels known for their higher calcium conductance during hyperpolarization, would better exhibit lysosomal exocytosis and measurable release of α-syn aggregates[92]. Furthermore, studies like ours that involve α-syn aggregate treatment add an additional layer of complexity. This is partially due to the ability of α-syn to alter the structural dynamics of actin, potentially inhibiting standard vesicular trafficking, and possibly even stabilizing cortical actin to physically hinder lysosomal access to the plasma membrane[93]. Ultimately, it is clear that our experimental approach to this mechanistic study of α-syn release will need to be refined substantially before accurate conclusions can be drawn.

CHAPTER SEVEN

CONCLUSIONS AND FUTURE DIRECTIONS

Although aspects of our study failed to produce conclusive evidence, there are multiple components of the colocalization analysis in **aim 2** that justify novel and interesting conclusions with respect to the intracellular trafficking of exogenous α-syn aggregates. First, this study builds on the largely debated previous evidence in favor of α-syn rupture as the mechanism of exogenous α-syn entry into the cytosol. Additionally, this study provides the first evidence suggesting that exogenous α-syn aggregates eventually accumulate within autolysosomes, along with overexpressed chGal3, after inducing rupture of endocytic vesicles. This conclusion is strongly supported by results of abundant and drastically enlarged triple positive puncta in our colocalization study, indicative of acidified vesicles containing cumulatively recruited α-syn^{+}/chGal3^{+} ruptured vesicles that may only be explained by mechanisms of macroautophagy. Moreover, accumulation within autolysosomes suggests that these degradative compartments are incapable of clearing accumulating α-syn. This could be a result of excessive treatment with α-syn aggregates, but is also likely to reflect ALP dysfunction. If α-syn is truly accumulating within autolysosomes as a result of dysfunction, then lysosomal exocytosis remains a key mechanism of α-syn release as a last line of defense by the cell.

Despite the lack of direct evidence of cathepsin B dispersion in this study, our model of cathepsin B dependent cell death after α-syn induced vesicle rupture is strengthened by this study. Based on our colocalization results, we can speculate that lysosomal disruption is occurring to the extent that substantial cathepsin release is

occurring, resulting in unregulated necrosis[55]. Perhaps in cases of PD, especially in early pathology, cells experience occasional, full rupture of lysosomes, causing release of cathepsin B and D to cause mild disruption of surrounding structures, mitochondrial permeabilization, and subsequent release of both Cyt-C and ROS. In later stages of PD when pathological forms of α-syn are more abundant, however, cell death may occur more rapidly through mechanisms of necrosis as a result of increased cathepsin release consistent with our results of drastic lysosomal rupture. Particularly in synucleinopathies with much faster disease progression and vastly more abundant synuclein inclusions, like DLB, perhaps unregulated necrosis of neural tissue is the predominant form of cell death as active cathepsins degrade essential proteins and cause widespread disturbances throughout the cell. In the future, confirmation of cathepsin B and D dispersion upon α-syn aggregate treatment will play an important role in confirming or disproving our hypothesis of α-syn toxicity.

FUTURE DIRECTIONS

In addition to pursuing conclusive results for our unresolved aims, many studies in the field of PD research have sparked our interest in beginning more expansive studies. To start, the Jankovic lab at the Baylor College of Medicine has published interesting and relevant results of autophagic function in the presence of mutant forms of α-syn aggregates. Their results suggest that some mutant forms of α-syn can strongly bind the lysosomal membrane antigen, lamp2a, to prevent fusion of autophagosomes to lysosomes, thereby inhibiting macroautophagy[94]. We believe this effect may be exclusive to particular mutant forms of α-syn, in which case, our results suggesting successful autolysosome formation in the presence of WT α-syn aggregates still stand, although functional degradation may be inhibited due to saturation of the ALP pathway and

resulting strain on degradative machinery. Future studies investigating the ability of WT α-syn aggregates to bind lamp2a, however, may be warranted to verify our findings.

We also plan to further investigate cell response to α-syn treatment from the perspective of lysosomal synthesis. Evidence from the Björklund lab at Lund University suggests the lysosomal synthesis regulator, TFEB, is capable of enhancing autophagy when overexpressed to reduce pathological features of PD in rat models and ex-vivo human PD midbrains. The reverse effect was seen in TFEB deficient samples, in which neurotoxicity was increased. We would like to build upon these finding by investigating the effect of TFEB overexpression on α-syn intracellular trafficking, release, and chGal3 labeled rupture.

Eventually, we also hope to expand upon the chGal3 rupture assay by investigating the potential role of Galectin-3 in cellular recognition of, and response to, α-syn induced vesicle rupture. It has been determined that Galectin-3 plays a major role in inflammation and immunity[95]. Observations of Galectin-3 release from cells, and co-involvement in α-syn induced microglia activation have also been reported[96]. For these reasons, we suspect that there is likely an evolutionary reason for endogenous Galectin-3 to possess a C-terminal carbohydrate recognition domain capable of inducing relocalization of Galectin-3 to sites of vesicle rupture. Perhaps Galectin-3 is essential for the activation of the numerous neuroinflammatory changes that are activated in PD to induce toxicity[97]. We are anxious to conduct studies in the future investigating Galectin-3 as a component of LB and LN structures, contributor to α-syn toxicity, and even effector of α-syn release.

REFERENCES

1. Lee H-J, Bae E-J, Lee S-J. Extracellular α--synuclein-a novel and crucial factor in Lewy body diseases. *Nat Rev Neurol*. 2014;10(2):92-98. doi:10.1038/nrneurol.2013.275.
2. Spillantini MG, Schmidt ML, Lee VM, Trojanowski JQ, Jakes R, Goedert M. Alpha-synuclein in Lewy bodies. *Nature*. 1997;388(6645):839-840. doi:10.1038/42166.
3. Hansen C, Angot E, Bergström A-L, et al. α-Synuclein propagates from mouse brain to grafted dopaminergic neurons and seeds aggregation in cultured human cells. *J Clin Invest*. 2011;121(2):715-725. doi:10.1172/JCI43366.
4. Steiner J a, Angot E, Brundin P. A deadly spread: cellular mechanisms of α-synuclein transfer. *Cell Death Differ*. 2011;18(9):1425-1433. doi:10.1038/cdd.2011.53.
5. Lee H-J, Suk J-E, Bae E-J, Lee J-H, Paik SR, Lee S-J. Assembly-dependent endocytosis and clearance of extracellular alpha-synuclein. *Int J Biochem Cell Biol*. 2008;40(9):1835-1849. doi:10.1016/j.biocel.2008.01.017.
6. Varkey J, Isas JM, Mizuno N, et al. Membrane curvature induction and tubulation are common features of synucleins and apolipoproteins. *J Biol Chem*. 2010;285(42):32486-32493. doi:10.1074/jbc.M110.139576.
7. Freeman D, Cedillos R, Choyke S, et al. Alpha-Synuclein Induces Lysosomal Rupture and Cathepsin Dependent Reactive Oxygen Species Following Endocytosis. Kahle PJ, ed. *PLoS One*. 2013;8(4):e62143. doi:10.1371/journal.pone.0062143.
8. Lewy, Frederick H. Lewandowski M. No Titl. In: *Handbuch Der Neurologie Band III*. Berlin; 1912:920-933.
9. Tretiakoff MC. No Title. 1919.
10. Okazaki H, Lipkin LE, Aronson SM. No Title. *J Neuropathol*. 1961;20:237-244.
11. Kosaka K, Oyanagi S, Matsushita M, Hori A, Iwase S. No Title. *Acta Neuropathol*. 1976;36:221-233.
12. McKeith IG, Galasko D, Kosaka K, et al. Consensus guidelines for the clinical and pathologic diagnosis of dementia with Lewy bodies (DLB): report of the consortium on DLB international workshop. *Neurology*. 1996;47(5):1113-1124. doi:10.1212/WNL.47.5.1113.
13. Yoshida M. Multiple system atrophy: a-synuclein and neuronal degeneration. *Neuropathology*. 2007;27(5):484-493. doi:10.1111/j.1440-1789.2007.00841.x.
14. Braak H, Del Tredici K, Rüb U, De Vos RAI, Jansen Steur ENH, Braak E. Staging of brain pathology related to sporadic Parkinson's disease. *Neurobiol Aging*. 2003;24(2):197-211. doi:10.1016/S0197-4580(02)00065-9.
15. Papp MI, Kahn JE, Lantos PL, et al. Glial cytoplasmic inclusions in the CNS of patients with multiple system atrophy (striatonigral degeneration, olivopontocerebellar atrophy and Shy-Drager syndrome). *J Neurol Sci*. 1989;94(1-3):79-100. doi:10.1016/0022-510X(89)90219-0.
16. Papapetropoulos S, Tuchman A, Laufer D, Papatsoris AG, Papapetropoulos N, Mash DC. Causes of death in multiple system atrophy. *J Neurol Neurosurg Psychiatry*. 2007;78(3):327-329. doi:10.1136/jnnp.2006.103929.

17. Glass GA, Josephs KA, Ahlskog JE, et al. Respiratory Insufficiency as the Primary Presenting Symptom of Multiple-System Atrophy. *Arch Neurol*. 2006;63(7):978. doi:10.1001/archneur.63.7.978.
18. Mccann H, Cartwright H, Halliday GM. Neuropathology of α-synuclein propagation and braak hypothesis. *Mov Disord*. 2015;00(00):1-9. doi:10.1002/mds.26421.
19. Savica R, Grossardt BR, Bower JH, Ahlskog JE, Rocca WA. Incidence and pathology of synucleinopathies and tauopathies related to parkinsonism. *JAMA Neurol*. 2013;70(7):859-866. doi:10.1001/jamaneurol.2013.114.
20. Doty RL. Olfactory dysfunction in Parkinson disease. *Nat Rev Neurol*. 2012;8(6):329-339. doi:10.1038/nrneurol.2012.80.
21. Dodel R, Csoti I, Ebersbach G, et al. Lewy body dementia and Parkinson's disease with dementia. *J Neurol*. 2008;255(SUPPL. 5):39-47. doi:10.1007/s00415-008-5007-0.
22. Edison P, Rowe CC, Rinne JO, et al. Amyloid load in Parkinson's disease dementia and Lewy body dementia measured with [11C]PIB positron emission tomography. *J Neurol Neurosurg Psychiatry*. 2008;79(12):1331-1338. doi:10.1136/jnnp.2007.127878.
23. Steenland K, MacNeil J, Seals R, Levey A. Factors affecting survival of patients with neurodegenerative disease. *Neuroepidemiology*. 2010;35(1):28-35. doi:10.1159/000306055.
24. Lloyd KG, Davidson L, Hornykiewicz O. The neurochemistry of Parkinson's disease: effect of L-dopa therapy. *J Pharmacol Exp Ther*. 1975;195(3):453-464. doi:VL - 195.
25. Rocha S, Monteiro A, Linhares P, et al. Long-term mortality analysis in Parkinson's disease treated with deep brain stimulation. *Parkinsons Dis*. 2014;2014:1-5. doi:10.1155/2014/717041.
26. Klingelhoefer L, Samuel M, Chaudhuri KR, Ashkan K. An update of the impact of deep brain stimulation on non motor symptoms in Parkinson's disease. *J Parkinsons Dis*. 2014;4(2):289-300. doi:10.3233/JPD-130273.
27. Kordower JH, Chu Y, Hauser RA, Olanow CW, Freeman TB. Transplanted dopaminergic neurons develop PD pathologic changes: a second case report. *Mov Disord*. 2008;23(16):2303-2306. doi:10.1002/mds.22369.
28. Beach TG, Adler CH, Sue LI, et al. Multi-organ distribution of phosphorylated α-synuclein histopathology in subjects with Lewy body disorders. *Acta Neuropathol*. 2010;119(6):689-702. doi:10.1007/s00401-010-0664-3.
29. Iwai A, Masliah E, Yoshimoto M, et al. The precursor protein of non-Aβ component of Alzheimer's disease amyloid is a presynaptic protein of the central nervous system. *Neuron*. 1995;14(2):467-475. doi:10.1016/0896-6273(95)90302-X.
30. Maroteaux L, Scheller RH. The rat brain synucleins; family of proteins transiently associated with neuronal membrane. *Mol Brain Res*. 1991;11(3):335-343. doi:10.1016/0169-328X(91)90043-W.
31. Maroteaux L, Campanelli JT, Scheller RH. Synuclein: a neuron-specific protein localized to the nucleus and presynaptic nerve terminal. *J Neurosci*. 1988;8(8):2804-2815. http://www.ncbi.nlm.nih.gov/pubmed/3411354. Accessed

May 8, 2016.
32. Eliezer D, Kutluay E, Bussell R, Browne G. Conformational properties of α-synuclein in its free and lipid-associated states. *J Mol Biol*. 2001;307(4):1061-1073. doi:10.1006/jmbi.2001.4538.
33. Burré J, Sharma M, Südhof TC. α-Synuclein assembles into higher-order multimers upon membrane binding to promote SNARE complex formation. *Proc Natl Acad Sci U S A*. 2014;111(40):E4274-E4283. doi:10.1073/pnas.1416598111.
34. Anderson JP, Walker DE, Goldstein JM, et al. Phosphorylation of Ser-129 is the dominant pathological modification of a-synuclein in familial and sporadic lewy body disease. *J Biol Chem*. 2006;281(40):29739-29752. doi:10.1074/jbc.M600933200.
35. Spillantini MG. a-Synuclein in filamentous inclusions of Lewy bodies from Parkinson ' s disease and dementia with Lewy bodies. 1998;95(May):6469-6473.
36. Serpell LC, Berriman J, Jakes R, Goedert M, Crowther RA. Fiber diffraction of synthetic alpha-synuclein filaments shows amyloid-like cross-beta conformation. *Proc Natl Acad Sci U S A*. 2000;97(9):4897-4902. http://www.ncbi.nlm.nih.gov/pubmed/10781096. Accessed May 13, 2016.
37. Miake H, Mizusawa H, Iwatsubo T, Hasegawa M. Biochemical characterization of the core structure of a-synuclein filaments. *J Biol Chem*. 2002;277(21):19213-19219. doi:10.1074/jbc.M110551200.
38. Singleton a B, Farrer M, Johnson J, et al. alpha-Synuclein locus triplication causes Parkinson's disease. *Science*. 2003;302(5646):841. doi:10.1126/science.1090278.
39. Chartier-Harlin M-CC, Kachergus J, Roumier C, et al. α-synuclein locus duplication as a cause of familial Parkinson's disease. *Lancet*. 2004;364(9440):1167-1169. doi:10.1016/S0140-6736(04)17103-1.
40. Borghi R, Marchese R, Negro A, et al. *Full Length α-Synuclein Is Present in Cerebrospinal Fluid from Parkinson's Disease and Normal Subjects*. Vol 287.; 2000. doi:10.1016/S0304-3940(00)01153-8.
41. El-Agnaf OMA, Salem SA, Paleologou KE, et al. Alpha-synuclein implicated in Parkinson's disease is present in extracellular biological fluids, including human plasma. *FASEB J*. 2003;17(13):1945-1947. doi:10.1096/fj.03-0098fje.
42. Lee PH, Lee G, Park HJ, Bang OY, Joo IS, Huh K. The plasma alpha-synuclein levels in patients with Parkinson's disease and multiple system atrophy. *J Neural Transm*. 2006;113(10):1435-1439. doi:10.1007/s00702-005-0427-9.
43. Ben GT, Loeb V, Israeli E, Altschuler Y, Selkoe DJ, Sharon R. Alpha-synuclein and polyunsaturated fatty acids promote clathrin mediated endocytosis and synaptic vesicle recycling. *Traffic*. 2009;10(2):218-234. doi:10.1111/j.1600-0854.2008.00853.x.
44. Maier O, Marvin SA, Wodrich H, Campbell EM, Wiethoff CM. Spatiotemporal Dynamics of Adenovirus Membrane Rupture and Endosomal Escape. *J Virol*. 2012;86(19):10821-10828. doi:10.1128/JVI.01428-12.
45. Maejima I, Takahashi A, Omori H, et al. Autophagy sequesters damaged lysosomes to control lysosomal biogenesis and kidney injury. *EMBO J*. 2013;32(17):2336-2347. doi:10.1038/emboj.2013.171.
46. Paz I, Sachse M, Dupont N, et al. Galectin-3, a marker for vacuole lysis by invasive pathogens. *Cell Microbiol*. 2010;12(4):530-544. doi:10.1111/j.1462-

5822.2009.01415.x.
47. Wiethoff CM, Wodrich H, Gerace L, Nemerow GR. Adenovirus Protein VI Mediates Membrane Disruption following Capsid Disassembly Adenovirus Protein VI Mediates Membrane Disruption following Capsid Disassembly. *J Virol*. 2005;79(4):1992-2000. doi:10.1128/JVI.79.4.1992.
48. Rhoades E, Ramlall TF, Webb WW, Eliezer D. Quantification of alpha-synuclein binding to lipid vesicles using fluorescence correlation spectroscopy. *Biophys J*. 2006;90(12):4692-4700. doi:10.1529/biophysj.105.079251.
49. Breydo L, Wu JW, Uversky VN. α-Synuclein misfolding and Parkinson's disease. *Biochim Biophys Acta - Mol Basis Dis*. 2012;1822(2):261-285. doi:10.1016/j.bbadis.2011.10.002.
50. Dikiy I, Eliezer D. Folding and misfolding of alpha-synuclein on membranes. *Biochim Biophys Acta*. 2012;1818(4):1013-1018. doi:10.1016/j.bbamem.2011.09.008.
51. Codolo G, Plotegher N, Pozzobon T, et al. Triggering of inflammasome by aggregated α-synuclein, an inflammatory response in synucleinopathies. *PLoS One*. 2013;8(1):e55375. doi:10.1371/journal.pone.0055375.
52. Brustovetsky N, Dubinsky JM, Antonsson B, Jemmerson R. Two pathways for tBID-induced cytochrome c release from rat brain mitochondria: BAK- versus BAX-dependence. *J Neurochem*. 2002;84(1):196-207. doi:10.1046/j.1471-4159.2003.01545.x.
53. Zhang H, Zhong C, Shi L, Guo Y, Fan Z. Granulysin induces cathepsin B release from lysosomes of target tumor cells to attack mitochondria through processing of bid leading to Necroptosis. *J Immunol*. 2009;182(11):6993-7000. doi:10.4049/jimmunol.0802502.
54. Bidère N, Lorenzo HK, Carmona S, et al. Cathepsin D triggers Bax activation, resulting in selective apoptosis-inducing factor (AIF) relocation in T lymphocytes entering the early commitment phase to apoptosis. *J Biol Chem*. 2003;278(33):31401-31411. doi:10.1074/jbc.M301911200.
55. Guicciardi ME, Leist M, Gores GJ. Lysosomes in cell death. *Oncogene*. 2004;23(16):2881-2890. doi:10.1038/sj.onc.1207512.
56. Guicciardi ME, Deussing J, Miyoshi H, et al. Cathepsin B contributes to TNF-alpha-mediated hepatocyte apoptosis by promoting mitochondrial release of cytochrome c. *J Clin Invest*. 2000;106(9):1127-1137. doi:10.1172/JCI9914.
57. Turk V, Stoka V, Vasiljeva O, et al. Cysteine cathepsins: From structure, function and regulation to new frontiers. *Biochim Biophys Acta - Proteins Proteomics*. 2012;1824(1):68-88. doi:10.1016/j.bbapap.2011.10.002.
58. Buck MR, Karustis DG, Day NA, Honn K V, Sloane BF. Degradation of extracellular-matrix proteins by human cathepsin B from normal and tumour tissues. *Biochem J*. 1992;282 (Pt 1:273-278. http://www.pubmedcentral.nih.gov/articlerender.fcgi?artid=1130919&tool=pmcentrez&rendertype=abstract.
59. Lutgens SPM, Cleutjens KBJM, Daemen MJAP, Heeneman S. Cathepsin cysteine proteases in cardiovascular disease. *FASEB J*. 2007;21(12):3029-3041. doi:10.1096/fj.06-7924com.
60. Perfeito R, L??zaro DF, Outeiro TF, Rego AC. Linking alpha-synuclein

phosphorylation to reactive oxygen species formation and mitochondrial dysfunction in SH-SY5Y cells. *Mol Cell Neurosci*. 2014;62(SEPTEMBER):51-59. doi:10.1016/j.mcn.2014.08.002.

61. Fujiwara H, Hasegawa M, Dohmae N, et al. α-Synuclein is phosphorylated in synucleinopathy lesions. *Nat Cell Biol*. 2002;4(2):160-164. doi:10.1038/ncb748.
62. Tofaris GK. Lysosome-dependent pathways as a unifying theme in Parkinson's disease. *Mov Disord*. 2012;27(11):1364-1369. doi:10.1002/mds.25136.
63. Winklhofer KF, Haass C. Mitochondrial dysfunction in Parkinson's disease. *Biochim Biophys Acta - Mol Basis Dis*. 2010;1802(1):29-44. doi:10.1016/j.bbadis.2009.08.013.
64. Norris KL, Hao R, Chen L-F, et al. Convergence of Parkin, PINK1, and α-Synuclein on Stress-induced Mitochondrial Morphological Remodeling. *J Biol Chem*. 2015;290(22):13862-13874. doi:10.1074/jbc.M114.634063.
65. Angot E, Steiner JA, Lema Tomé CM, et al. Alpha-Synuclein Cell-to-Cell Transfer and Seeding in Grafted Dopaminergic Neurons In Vivo. Mosley RL, ed. *PLoS One*. 2012;7(6):e39465. doi:10.1371/journal.pone.0039465.
66. Wood SJ, Wypych J, Steavenson S, Louis J, Citron M, Biere AL. a-Synuclein Fibrillogenesis is Nucleation-dependent. *Biochemistry*. 1999:19509-19512.
67. Desplats P, Lee H-J, Bae E-J, et al. Inclusion formation and neuronal cell death through neuron-to-neuron transmission of alpha-synuclein. *Proc Natl Acad Sci U S A*. 2009;106(31):13010-13015. doi:10.1073/pnas.0903691106.
68. Decressac M, Mattsson B, Lundblad M, Weikop P, Björklund A. Progressive neurodegenerative and behavioural changes induced by AAV-mediated overexpression of α-synuclein in midbrain dopamine neurons. *Neurobiol Dis*. 2012;45(3):939-953. doi:10.1016/j.nbd.2011.12.013.
69. Lee H-J, Cho E-D, Lee KW, Kim J-H, Cho S-G, Lee S-J. Autophagic failure promotes the exocytosis and intercellular transfer of α-synuclein. *Exp Mol Med*. 2013;45(5):e22. doi:10.1038/emm.2013.45.
70. Lee H-J, Patel S, Lee S-J. Intravesicular Localization and Exocytosis of α-Synuclein and its Aggregates. *J Neurosci*. 2005;25(25):6016-6024. doi:10.1523/JNEUROSCI.0692-05.2005.
71. Ramakrishnan NA, Drescher MJ, Drescher DG. The SNARE complex in neuronal and sensory cells. *Mol Cell Neurosci*. 2012;50(1):58-69. doi:10.1016/j.mcn.2012.03.009.
72. Hutagalung AH, Novick PJ. Role of Rab GTPases in membrane traffic and cell physiology. *Physiol Rev*. 2011;91(1):119-149. doi:10.1152/physrev.00059.2009.
73. Jaiswal JK, Andrews NW, Simon SM. Membrane proximal lysosomes are the major vesicles responsible for calcium-dependent exocytosis in nonsecretory cells. *J Cell Biol*. 2002;159(4):625-635. doi:10.1083/jcb.200208154.
74. Caler E V., De Avalos SV, Haynes PA, Andrews NW, Burleigh BA. Oligopeptidase B-dependent signaling mediates host cell invasion by Trypanosoma cruzi. *EMBO J*. 1998;17(17):4975-4986. doi:10.1093/emboj/17.17.4975.
75. Ayala BP, Vasquez B, Clary S, Tainer JA, Rodland K, So M. The pilus-induced Ca 21 flux triggers lysosome exocytosis and increases the amount of Lamp1 accessible to Neisseria IgA1 protease. *Cell Microbiol*. 2001;3(4):265-275.

doi:10.1046/j.1462-5822.2001.00112.x.
76. Reddy A, Caler E V., Andrews NW. Plasma membrane repair is mediated by Ca2+-regulated exocytosis of lysosomes. *Cell*. 2001;106(2):157-169. doi:10.1016/S0092-8674(01)00421-4.
77. Rao SK, Huynh C, Proux-Gillardeaux V, Galli T, Andrews NW. Identification of SNAREs Involved in Synaptotagmin VII-regulated Lysosomal Exocytosis. *J Biol Chem*. 2004;279(19):20471-20479. doi:10.1074/jbc.M400798200.
78. Xu J, Toops K a., Diaz F, et al. Mechanism of polarized lysosome exocytosis in epithelial cells. *J Cell Sci*. 2012:5937-5943. doi:10.1242/jcs.109421.
79. Apetri MM, Harkes R, Subramaniam V, Canters GW, Schmidt T, Aartsma TJ. Direct Observation of α-Synuclein Amyloid Aggregates in Endocytic Vesicles of Neuroblastoma Cells. *PLoS One*. 2016;11(4):e0153020. doi:10.1371/journal.pone.0153020.
80. Mak SK, McCormack AL, Manning-Bog AB, Cuervo AM, Di Monte DA. Lysosomal degradation of alpha-synuclein in vivo. *J Biol Chem*. 2010;285(18):13621-13629. doi:10.1074/jbc.M109.074617.
81. Emmanouilidou E, Melachroinou K, Roumeliotis T, et al. Cell-produced alpha-synuclein is secreted in a calcium-dependent manner by exosomes and impacts neuronal survival. *J Neurosci*. 2010;30(20):6838-6851. doi:10.1523/JNEUROSCI.5699-09.2010.
82. Volpicelli-Daley LA, Luk KC, Patel TP, et al. Exogenous α-Synuclein Fibrils Induce Lewy Body Pathology Leading to Synaptic Dysfunction and Neuron Death. doi:10.1016/j.neuron.2011.08.033.
83. Platt FM, Boland B, van der Spoel AC. Lysosomal storage disorders: The cellular impact of lysosomal dysfunction. *J Cell Biol*. 2012;199(5):723-734. doi:10.1083/jcb.201208152.
84. Ballabio A, Gieselmann V. Lysosomal disorders: From storage to cellular damage. *BBA - Mol Cell Res*. 2008;1793:684-696. doi:10.1016/j.bbamcr.2008.12.001.
85. Brojatsch J, Lima H, Kar AK, et al. A proteolytic cascade controls lysosome rupture and necrotic cell death mediated by lysosome-destabilizing adjuvants. *PLoS One*. 2014;9(6):1-9. doi:10.1371/journal.pone.0095032.
86. Rempel SA, Rosenblum ML, Mikkelsen T, et al. Cathepsin B expression and localization in glioma progression and invasion. *Cancer Res*. 1994;54(23):6027-6031. http://www.ncbi.nlm.nih.gov/pubmed/7954439. Accessed May 25, 2016.
87. Linke M, Herzog V, Brix K. Trafficking of lysosomal cathepsin B-green fluorescent protein to the surface of thyroid epithelial cells involves the endosomal/lysosomal compartment. *J Cell Sci*. 2002;115(Pt 24):4877-4889. doi:10.1242/jcs.00184.
88. Qian Peter Su WDQJBXDJYZJLLYYS. Vesicle Size Regulates Nanotube Formation in the Cell. *Sci Rep*. 2016;6.
89. Rusten TE, Lindmo K, Juhász G, et al. Programmed Autophagy in the Drosophila Fat Body Is Induced by Ecdysone through Regulation of the PI3K Pathway. *Dev Cell*. 2004;7(2):179-192. doi:10.1016/j.devcel.2004.07.005.
90. Bi GQ, Morris RL, Liao G, Alderton JM, Scholey JM, Steinhardt RA. Kinesin- and myosin-driven steps of vesicle recruitment for Ca2+-regulated exocytosis. *J Cell Biol*. 1997;138(5):999-1008. http://www.ncbi.nlm.nih.gov/pubmed/9281579.

Accessed May 29, 2016.
91. Rodríguez A, Webster P, Ortego J, Andrews NW. Lysosomes behave as Ca2+-regulated exocytic vesicles in fibroblasts and epithelial cells. *J Cell Biol*. 1997;137(1):93-104. http://www.ncbi.nlm.nih.gov/pubmed/9105039. Accessed June 8, 2016.
92. Chan CS, Guzman JN, Ilijic E, et al. "Rejuvenation" protects neurons in mouse models of Parkinson's disease. *Nature*. 2007;447(7148):1081-1086. doi:10.1038/nature05865.
93. Sousa VL, Bellani S, Giannandrea M, et al. α-Synuclein and Its A30P Mutant Affect Actin Cytoskeletal Structure and Dynamics. *Mol Biol Cell*. 2009;20(16):3725-3739. doi:10.1091/mbc.E08-03-0302.
94. Pan T, Kondo S, Le W, Jankovic J. The role of autophagy-lysosome pathway in neurodegeneration associated with Parkinson's disease. *Brain*. 2008;131(8):1969-1978. doi:10.1093/brain/awm318.
95. Liu FT, Hsu DK, Zuberi RI, Kuwabara I, Chi EY, Henderson WR. Expression and function of galectin-3, a beta-galactoside-binding lectin, in human monocytes and macrophages. *Am J Pathol*. 1995;147(4):1016-1028. http://www.ncbi.nlm.nih.gov/pubmed/7573347. Accessed June 7, 2016.
96. Boza-Serrano A, Reyes JF, Rey NL, et al. The role of Galectin-3 in α-synuclein-induced microglial activation. *Acta Neuropathol Commun*. 2014;2(1):156. doi:10.1186/s40478-014-0156-0.
97. Blandini F. Neural and immune mechanisms in the pathogenesis of Parkinson's disease. *J Neuroimmune Pharmacol*. 2013;8(1):189-201. doi:10.1007/s11481-013-9435-y.

VITA

Zachary Carpenter Green grew up in Denver, CO. He discovered his interest in biomedical sciences and healthcare during his time at Columbine High School, which led him to declare a major in Integrative Physiology at the University of Colorado Boulder where he earned his Bachelor's degree in 2013. During his time at CU, Zach narrowed his research interests to neurodegeneration.

In the fall of 2014, Zach began studying Neuroscience as a master's student at Loyola University Chicago. Under the guidance of Dr. Edward Campbell, he has investigated the mechanisms behind neuronal death and disease progression in Parkinson's disease. He plans to apply knowledge gained from his graduate research experience to clinical research during his time at Chicago Medical School, which he will begin in August of 2016.